Journal of Nuclear Materials 596 (2024) 155121

Contents lists available at ScienceDirect

Journal of Nuclear Materials

journal homepage: www.elsevier.com/locate/jnucmat

Corrosion tests on austenitic samples with alumina and alumina-forming coatings in oxygen-containing stagnant Pb and turbulently flowing PbBi

Annette Heinzel [a,*], Renate Fetzer [a], Fabian Lang [a], Alfons Weisenburger [a], Sebastiano Cataldo [b], Fabio Di Fonzo [c], Georg Müller [a]

[a] Karlsruhe Institute of Technology (KIT), Institute for Pulsed Power and Microwave Technology (IHM), Hermann-von-Helmholtz-Platz 1, 76344, Eggenstein-Leopoldshafen, Germany
[b] Italian National Agency for New Technologies, Energy and Sustainable Economic Development (ENEA), „Brasimone" Research Centre, 40032, Camugnano, Bologna, Italy
[c] Centre for Nano-Science and Technology of the Italian Institute of Technology (IIT), Via Morego, 30 16163, Genova, Italy

HIGHLIGHTS

- 10,000 h tests proves the stability of alumina and alumina forming coatings in Pb.
- GIXRD shows formation of $Pb(Al_2O_4)$ on Al_2O_3 PLD coating.
- corrosion-erosion test in turbulent flowing LBE on alumina and forming coatings.

ARTICLE INFO

Keywords:
Coating
Liquid LBE
Liquid lead
Liquid metal corrosion

ABSTRACT

Two differently produced alumina coatings (by pulsed laser deposition (PLD) and detonation gun (DG)) and one alumina-forming coating realised by pack cementation are proposed as a protection barrier against corrosion of austenitic steels in Pb and PbBi. Samples were tested in oxygen-controlled stagnant Pb (10^{-7} wt.%) at 480 °C and 550 °C for up to 10,000 h and in turbulently flowing (up to 1.6 m/s) PbBi eutectic at 490 °C with 10^{-9}–10^{-8} wt. % oxygen for about 500 h. All exposed coatings showed a good behaviour in flowing PbBi and in stagnant Pb at around 480 °C independent of the oxygen content. At 550 °C, the PLD coating failed most probably due to incomplete coating of the sample, while the DG sample protected the base material.

1. Introduction

Heavy liquid metals (HLMs) such as lead or lead bismuth eutectic (LBE) have been proposed as heat transfer fluids and storage media in advanced nuclear and concentrating solar power systems [1–4]. One of the main drawbacks in the development of these systems is the solubility of alloying elements of structural steels, especially Ni and Cr, in the liquid metal at elevated temperatures. This leads to dissolution attack combined with liquid metal penetration, structural and phase changes (ferritization of austenitic steels), degradation of the mechanical properties and increased erosion [5]. The main approach to mitigate HLM corrosion is to support the in-situ formation of stable and protective oxide layers on the steel surface by dissolved oxygen in the HLM. Results of previous investigations show that depending on the surface and operation condition austenitic steels form either a duplex layered oxide, which consists of an outer layer of magnetite (Fe_3O_4) and an inner layer of spinel ($Fe(Fe_xCr_{1-x})_2O_4$), or a single layer oxide of ($Fe(Fe_xCr_{1-x})_2O_4$) or Cr-oxide. However, the highest temperature for protection of austenitic steel by these in-situ grown oxide scales is 500 °C [5]. For higher temperatures, these oxide layers are not protective anymore and dissolution attack is observed [5,6]. One possibility to achieve material compatibility at higher operation temperatures is the application of protective surface coatings. Many coatings do not rely on the in-situ formation of protective oxide layers, which may allow a lower oxygen concentration during operation or fluctuating oxygen concentrations. A disadvantage is that they do not possess self-healing properties. Therefore, strong adhesion, structural integrity, chemical stability, and a high wear resistance are minimum requirements of coatings to be applied. To

* Corresponding author.
E-mail address: annette.heinzel@kit.edu (A. Heinzel).

https://doi.org/10.1016/j.jnucmat.2024.155121
Received 28 February 2023; Received in revised form 22 April 2024; Accepted 22 April 2024
Available online 23 April 2024

Table 1
Chemical composition (wt.%) of 316L [23] and 15-15Ti [24].

	Cr	W	Ni	Mn	V	Mo	Ti	Al	Cu	C	N	P	S	Si	Fe
316L	16.73	0.02	9.97	1.81	0.07	2.05	0.006	0.02	0.23	0.0185	0.029	0.032	0.0035	0.67	Bal.
15-15Ti	15.95	<0.005	15.40	1.49	0.036	1.20	0.44	0.023	0.026	0.1	0.009	<0.01	0.0036	0.52	Bal.

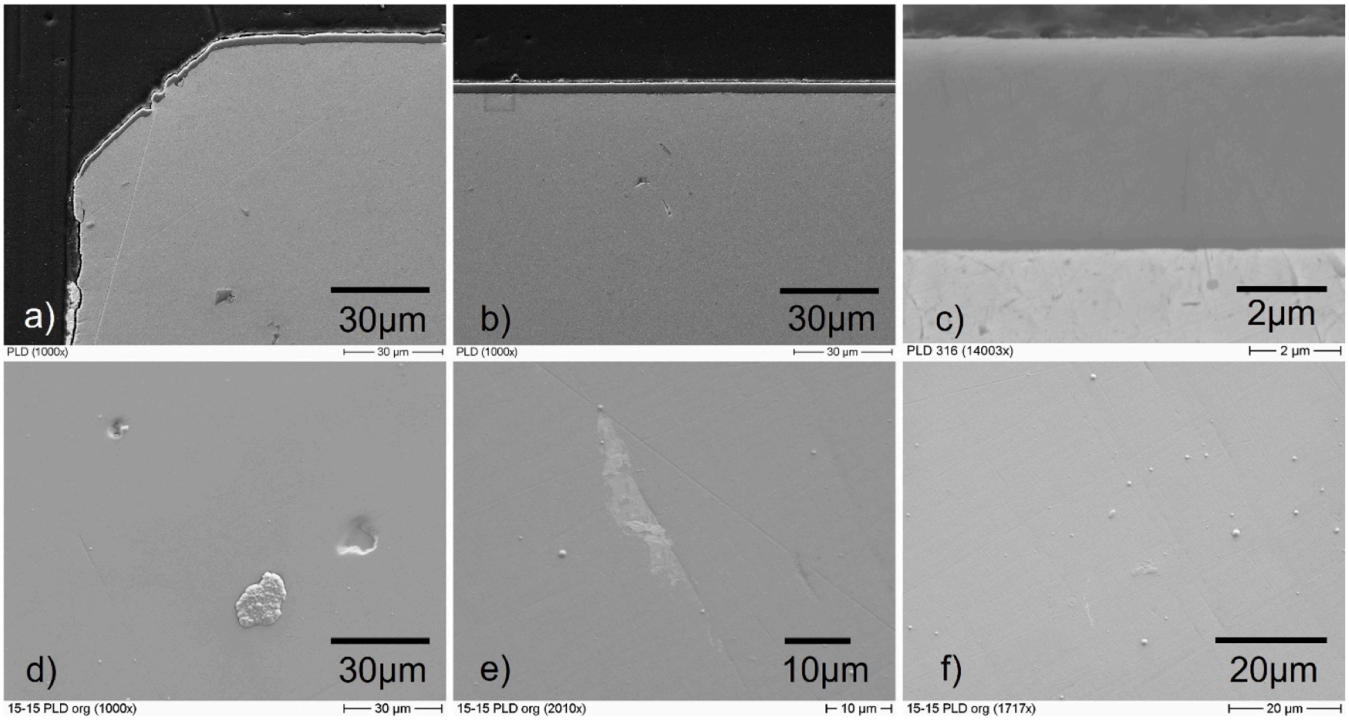

Fig. 1. SEM photos of a PLD sample: cross-section (a, b, c) and surface (d, e, f); substrate steel is 316L in (c) and 15-15Ti in all other cases.

be used on heat exchangers and cladding tubes, the coating has to be thin, should not degrade the thermal conductivity significantly, and has to be irradiation resistant.

In recent years, mainly amorphous Al_2O_3 coatings with few randomly distributed nanocrystalline α-Al_2O_3 grains produced by pulsed laser deposition (PLD) were tested on the basis of the above-mentioned criteria. The coating exhibits high resistance to thermal cycling, nano-impact and scratching [7–11]. Only the mechanical strength was found to be somewhat lower for the coated steel, most probably due to the coating process [11]. No liquid metal embrittlement was observed at 400 and 500 °C in Pb at strain rates of 5×10^{-5} s^{-1} and 5×10^{-6} s^{-1}, respectively [11]. Corrosion tests at 550 °C in oxygen-saturated Pb up to 500 h and in Pb with 10^{-8} wt.% oxygen up to 4000 h exhibited no interaction with the liquid metal under these conditions [8,9]. Even after 8000 h in dynamic Pb at 550 °C with 10^{-8}–10^{-7} wt.% oxygen up to 8000 h the coating was still compact and continuous, but it revealed a slight roughness with Pb enrichments directly at the surface [12]. Comparable investigations of these coatings in PbBi do not exist so far and are presented in this work.

Another possibility to apply an Al_2O_3 coating is thermal spraying by detonation gun (DG). This coating method is known to produce excellent alumina coatings with respect to hardness, wear-resistance, density, and adhesive strength [13,14], but they are usually thicker (50–500 µm) [15] than PLD coatings (only a few microns) and, therefore, more suitable for reactor components other than fuel cladding tubes and heat exchanger tubes. Tensile tests at 550 °C in LBE with an oxygen content of 10^{-13} wt.% showed that the coating is very stable and protective in the liquid metal at the tested temperature as long as it is not damaged mechanically [16]. Recently, some corrosion tests were conducted in dynamic Pb with 10^{-8}–10^{-7} wt.% oxygen with a duration up to 8000 h [12]. Surprisingly, the 2200 h sample showed Pb penetration up to the middle of the coating, which was not the case for the samples exposed for 4000 h and 8000 h. These samples exhibited a slight oxidation of the 15-15Ti base material at the coating/substrate interface. After 8000 h, microcracks appeared at the surface of the coating, which had apparently no negative impact.

Self-healing properties can be gained by adding strong oxide formers like Al and Si into the steel. A single, dense alumina layer can be formed in-situ during exposure with a sufficient oxygen content, especially at higher temperatures [17]. However, Al and Si degrade the mechanical properties, may change the behaviour of the steel under irradiation, and promote the formation of ferrite. Therefore, methods to add aluminium only into the steel surface are of interest, like pack cementation or GESA (pulsed electron beam facility) treatment. The latter alloys Al into the steel surface or alloys an Al containing metallic coating to a steel surface by melting with a pulsed electron beam [6,18]. GESA treated materials have been studied extensively in Pb and LBE with promising results [19–21]. Pack cementation coatings have been tested little. In Ref. [22], aluminized T91 and 316L steel were tested in dynamic (up to 2.3 m/s) and stagnant LBE. Most of the tests were carried out with an oxygen concentration below 10^{-8} wt.%. Even under these unfavourable conditions, the coating behaved well up to 500 °C. At higher temperature, corrosion and corrosion-erosion damage took place. At higher oxygen concentration (up to 10^{-6} wt.%), the coating behaved well even at 600 °C for 1000 h of exposure at laminar flow conditions.

In this present study, long-term corrosion tests (up to 10,000 h) in stagnant Pb and corrosion tests in turbulently flowing LBE (here denoted as PbBi) were conducted on two slightly different austenitic steels (316L

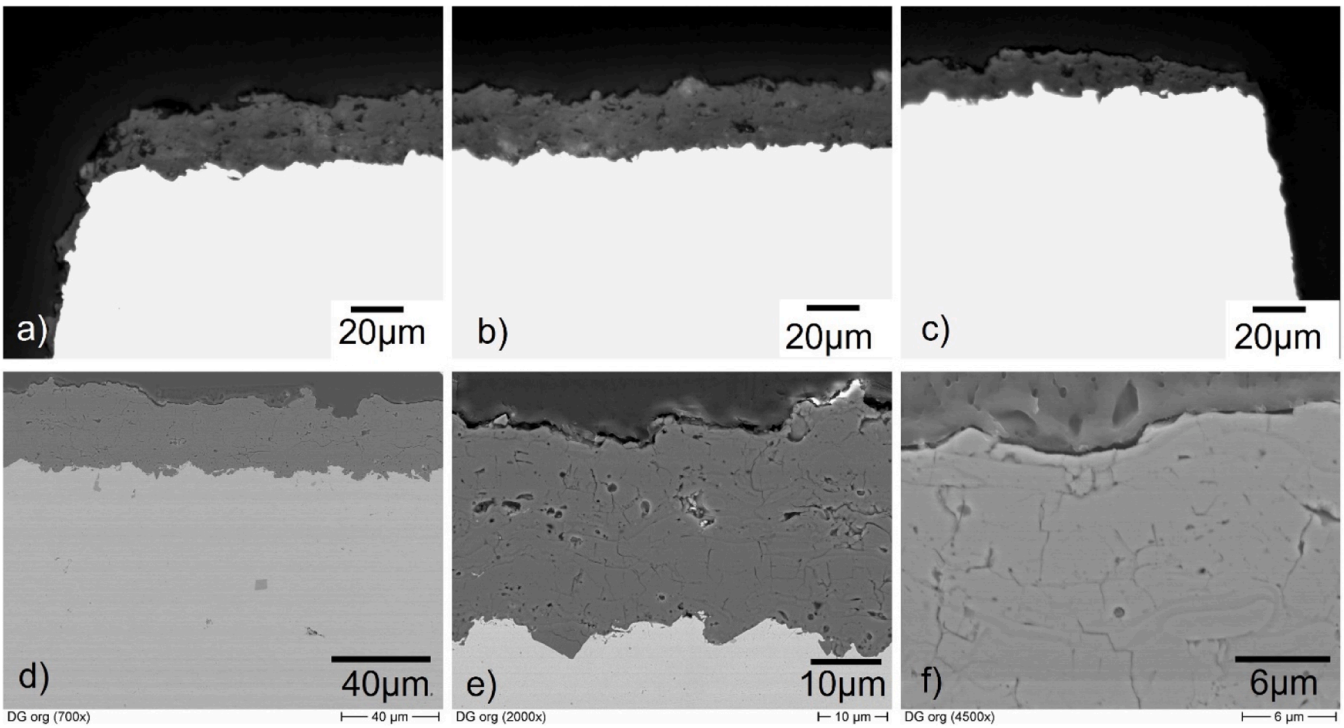

Fig. 2. a–c) LOM photos of the cross-section of the DG sample on 316L showing the decrease of the coating thickness from one side to the other and (d–f) SEM photos of the coating with a higher magnification showing the inhomogeneous structure with pores and cracks.

or 15-15Ti) with alumina coatings produced by pulsed laser deposition and detonation gun and an alumina-forming coating produced by pack cementation as corrosion protection. The long-term corrosion tests in stagnant Pb with 10^{-7} wt.% oxygen were performed at temperatures of 480 °C and 550 °C, respectively, which corresponds to the temperature and oxygen conditions foreseen in GenIV LFRs (lead-cooled fast reactors). The corrosion tests were carried out at 490 °C in flowing PbBi with an oxygen concentration in the range 10^{-9}–10^{-8} wt.%. The average PbBi flow velocity along the lateral surface of the samples was 0.3, 0.8, 1.4, and 1.6 m/s which are flow velocities relevant for ALFRED.

2. Experimental

2.1. Substrate materials

As substrate material, the two austenitic steels 316L and 15-15Ti (DIN/EN - 1.4970; only for PLD and DG) were chosen. Both materials are candidate materials for the European GEN-IV reactor ALFRED (Advanced Lead Fast Reactor Demonstrator) and for MYRRHA (Multi-purpose HYbrid Research Reactor for High-tech Applications). The 316L specimens were obtained from an industrial-size 316L steel heat, the EUROTRANS-DEMETRA heat, Industeel, ArcelorMittal Group (Luxembourg) [23]. The steel plate with a thickness of 15 mm was hot-rolled, solution-annealed at 1050–1100 °C, and water quenched. The 15-15Ti used in the current experiments, a rod material with a diameter of 40 mm, was solution-annealed at 1100 °C for 30 min. The chemical composition of these steels is reported in Table 1. All substrates were machined into flat coupons of 8 × 28 × 2 mm^3 (width × height × depth). Before the deposition of the alumina coating, the substrate surfaces were prepared by grinding and polishing. For PLD and pack cementation, the substrate surfaces were grinded with silicon carbide paper finally with grit size 1200, while the substrate surfaces for PLD were additionally polished finally with 1 µm diamond paste. Afterwards the samples were cleaned with ethanol in an ultrasonic bath. Substrate surfaces for the DG coating were sandblasted.

2.2. Coating deposition

Alumina coatings were deposited on austenitic steel substrates by three different coating technologies, pulsed laser deposition (PLD), detonation gun spray deposition (DG), and also by depositing an alumina-forming coating by pack-cementation.

2.1.1. PLD deposition

In the case of PLD, Al_2O_3 coatings of approximately 3 to 5 µm thickness were deposited on only one of the sample facets with parameters described in Ref. [7]. The deposition took place without addition heating of the sample. All PLD coatings were dense and characterised by uniform thickness (Fig. 1b, c) and mirror-like surface finished. The slightly bevelled edges were also covered by the coating, but the coating was thinner and partially discontinuous in these areas, Fig. 1a. SEM examinations of the surface reveal defects like in Fig. 1d–f. The small spheres, which can be seen on all three photos, are most probably droplets from the manufacturing process and consist as well of Al and oxygen. The presents of droplets are a typical feature of PLD coatings. Large droplets might lead to a loss of structural integrity of the coating during the test especially if the oxygen is able to diffuse around the droplets and to oxidize the steel material. The oxide growing on the steel surface can reach the surface of the coating and destroy locally the coating. Therefore, a quality test of the coating was done on one coated sample. It was put in a furnace with air and heated up to 550 °C, the temperature was held for 72 h and then cooled down. Examinations afterward showed that the droplets and defects were still there, together with some additional dots that also consist of Al and O, but neither cracks nor Fe-oxide from the base material could be detected. According to Ref. [7], the coating is expected to be mainly amorphous Al_2O_3 coating with few randomly distributed nanocrystalline α-Al_2O_3 grains. GIXRD (grazing incidence X-ray diffraction) patterns taken from the pristine coated sample showed only peaks from the base material, which confirms that the coating was predominantly amorphous with little to no crystallinity.

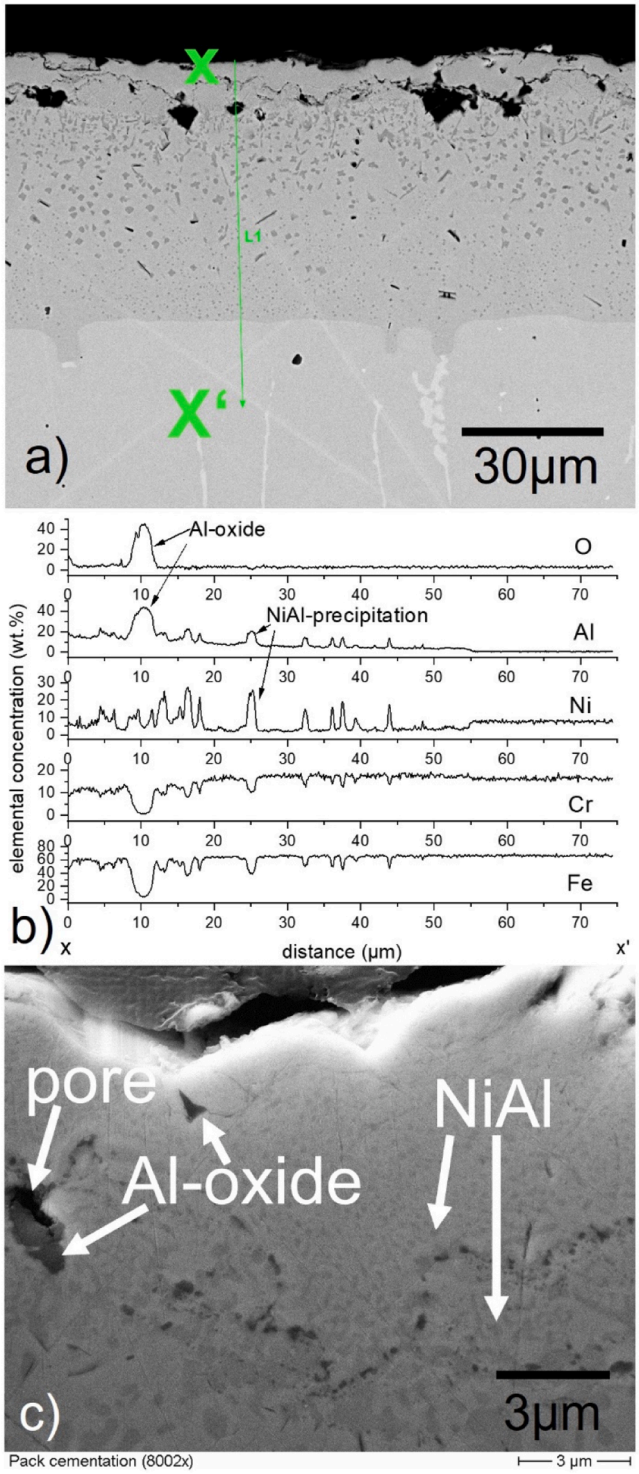

Fig. 3. a) SEM photo of the cross-section of the pack cementation sample (316L substrate) with EDS line scan b) measurement O, Al, Ni, Cr and Fe (wt.%) (Si, Mo, Mn was also measured, but forms no precipitations and is therefore not shown here); c) upper part of the coating with a higher magnification.

2.2.2. DG deposition

As a precursor in the DG process, Al_2O_3 powder (105NS, Oerlikon Metco; Switzerland) was used as received but dried overnight at 80 °C. For the DG deposition, a CCDS-2000 system (STPC Ltd., Novosibirsk, Russia) was used. The sandblasted substrate samples were mounted on the robotic sample holder arm of the instrument keeping a standstill distance from the gun of 10 cm. Then, while in translation, two layers of alumina were sprayed and deposited on the sample surface. The as-deposited samples appeared covered on the lateral flat surfaces with a coating thickness decreasing from one edge to the other (Fig. 2a–c), varying from about 28 µm at the left edge to about 17 µm at the right edge. This uniformly decreasing thickness was caused by a slight misalignment of the sample with respect to the spraying gun of the DG machine. The alumina coating showed a rough surface, which is a typical feature of thermal sprayed powder coatings. Between the interface and the coating was no gap observable. Photos of the cross-section with a higher magnification are depicted in Fig. 2d–f. They show an inhomogeneous structure with pores, stair-like cracks, and internal boundaries that often appear parallel to the substrate.

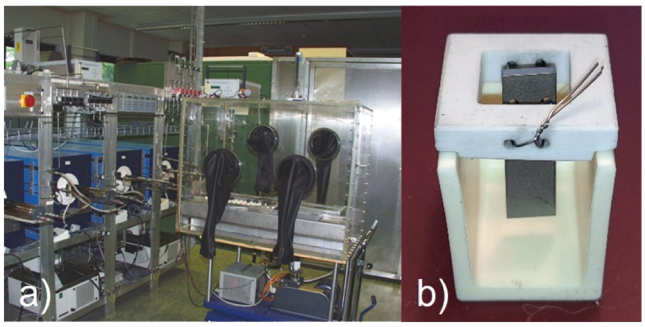

Fig. 4. a) COSTA facility with connected glovebox for sampling [26]; b) cut crucible with sample fixed on a sample holder.

2.2.3. Alumina-forming coatings

Alumina-forming coatings were produced by the company Lincotek Surface Solutions. For this purpose, the surface of 316L samples were aluminized by pack cementation. After aluminizing, the samples showed the around 50–58 µm thick typical Al pack-cementation layer. It consisted of a thin outer layer (~4–10 µm) with a higher amount of Al (on average around 14 wt.%) compared with the Al content of the much thicker inner layer, in which the Al amount gradually decreases towards the bulk (Al-diffusion layer), see SEM photo and line scan Fig. 3a, b. In the entire Al containing layer, Al and Ni formed precipitates that are visible as dark grey spots. They are very small (around 200 nm) in the outer thin layer (Fig. 3c). In the first 2/3 of the inner layer, the Al-Ni precipitations are larger (up to 2.5 µm) and then decrease in size toward the bulk material. The large black precipitations at the transition between the inner and outer layer and the black lines inside the outer layer are Al-oxides. Also, the larger black parts are Al-oxides as visible in the line scan. Additionally, bright precipitations with a higher Cr content are visible in the 316L base material. These are σ-phases, which were previously described in the same EUROTRANS-DEMETRA material batch [25].

2.3. Corrosion test facilities and test conditions

2.3.1. Corrosion tests in stagnant Pb (COSTA facility)

All corrosion tests were done in isothermal conditions. The corrosion tests in stagnant Pb were performed in the corrosion test facility COSTA (**CO**rrosion test stand for **ST**agnant liquid **A**lloys) [26], Fig. 4a), which consists of tubular furnaces with quartz tubes as reaction chambers and oxygen control systems. Inside the COSTA facility, alumina crucibles were placed on a crucible carrier for sampling. Each crucible was filled with 180–200 g Pb (99,94 %-delivered by Feinhütte Halsbrücke GmbH) so that more than 50 % of each sample was immersed in the liquid metal in one crucible, which led to a surface sample to Pb volume ratio of around 2.96 cm^2/0.0159 l (50 % immersed and 180 g Pb). In order to prevent floating of the samples, they were fixed in the upper part with Mo wires on alumina holders as demonstrated in Fig. 4b. The oxygen concentration in the liquid metal was controlled via the gas atmosphere

Table 2
Exposure time and temperature for the coated samples in stagnant lead and respective base material.

Pb / 10^{-7} wt.%	480 °C / 316L			550 °C / 15-15Ti		
	2000 h	6528 h	10,000 h	144 h	5000 h	10,000 h
Pulsed Laser deposition	x	x	x	x	x	X
Al_2O_3 Detonation Gun	x	x	x	–	x	X
Pack cementation	x	x	x	–	–	–

by establishing a defined H_2/H_2O ratio, which determines the chemical potential of oxygen in the liquid metal [27]. Based on the oxygen saturation data [28], the oxygen concentration in molten Pb was adjusted to 10^{-7} wt.%, because an oxygen content between 10^{-8} and 10^{-6} wt.% is foreseen for ALFRED [29]. The gas atmosphere was established by a continuous gas flow through the quartz tube and its oxygen partial pressure and moisture was continuously monitored after leaving the tube. The liquid metal was held for 1 week under test conditions to be sure that the envisaged oxygen content was adjusted. To immerse and to extract samples from molten Pb, a glovebox conditioned to the same oxygen partial pressure as the gas phase in the COSTA quartz tube was used to keep the oxygen condition stable. The samples were taken out from the glovebox after cooling down to room temperature for the post examination.

Table 2 shows the exposure time and temperature for the coated samples. The 316L was employed as substrate material at 480 °C, because 316L is at time foreseen as structural material for parts like the steam generator, the vessel, and the diaphragm where, under normal conditions, 480 °C should be the maximum operation temperature [29]. The 15-15Ti stabilized material however, is discussed as cladding material with an expected maximum temperature of 550 °C. Therefore, 15-15Ti served as substrate material for the coating tests at the higher temperature. The use of pack cementation is at time discussed only for the 316L and at regions with lower temperature and was therefore only applied to the 316L substrate materials.

2.3.2. *Corrosion tests in turbulently flowing PbBi (CORELLA facility)*

The corrosion tests in turbulently flowing PbBi were conducted in the CORELLA (CORrosion-Erosion test facility for Liquid Lead Alloy) test facility at KIT, in which specimens can be exposed to flowing liquid metals with a controlled oxygen content [30,31]. CORELLA consists of two chambers, one for conditioning the liquid PbBi to the desired oxygen content (based on the oxygen saturation data [28]) and the other for the exposure experiment. A rotating inner cylinder generates the flow of the liquid metal in the cylindrical exposure chamber, see Fig. 5a, b. The chamber is covered by a gas-tight lid. Below the lid a sample holder plate is placed, on which up to 6 samples can be fixed. After filling the chamber with ~9.6 l PbBi the specimens are fully immersed, even under rotation. The velocity of the PbBi around the specimens is controlled by

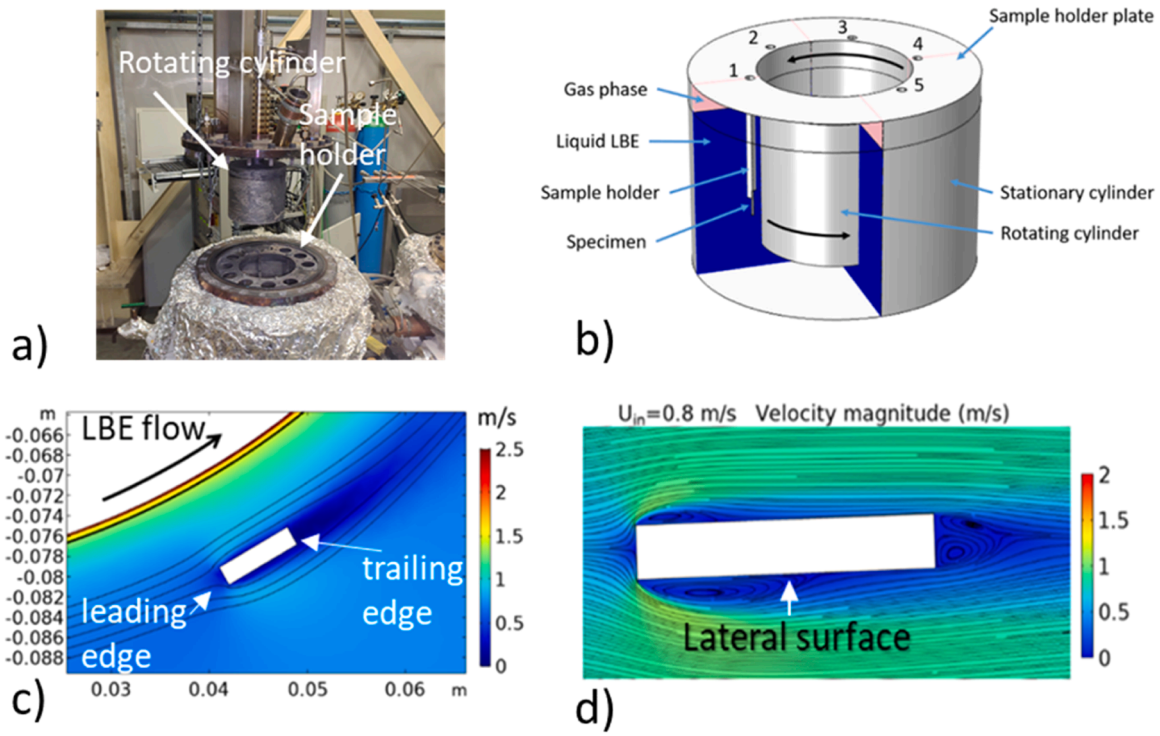

Fig. 5. a, b) Exposure chamber of CORELLA test facility (b) with 5 pairs of sample holders and specimens inserted; c) Visualization of flow field on exemplary horizontal cross-section; d) Result of high-resolution simulation of flow around one specimen. c) and d) show the velocity magnitude as colour map and streamlines.

Table 3
Exposed samples and test conditions.

Samples	Substrate material	Test condition [rpm]	Average speed along lateral surfaces	Temperature [°C]	Exposure time [h]	Oxygen condition [wt.%] (most of the time)
Detonation gun	316	200	0.3 m/s	490	480	~2×10^{-9}
Pulsed Laser	316	500	0.8 m/s	490	480	2×10^{-9}–7×10^{-9}
Deposition	15-15Ti	1000	1.4 m/s	490	500	~2×10^{-9}
	15-15Ti	1200	1.6 m/s	490	480	~2×10^{-9}

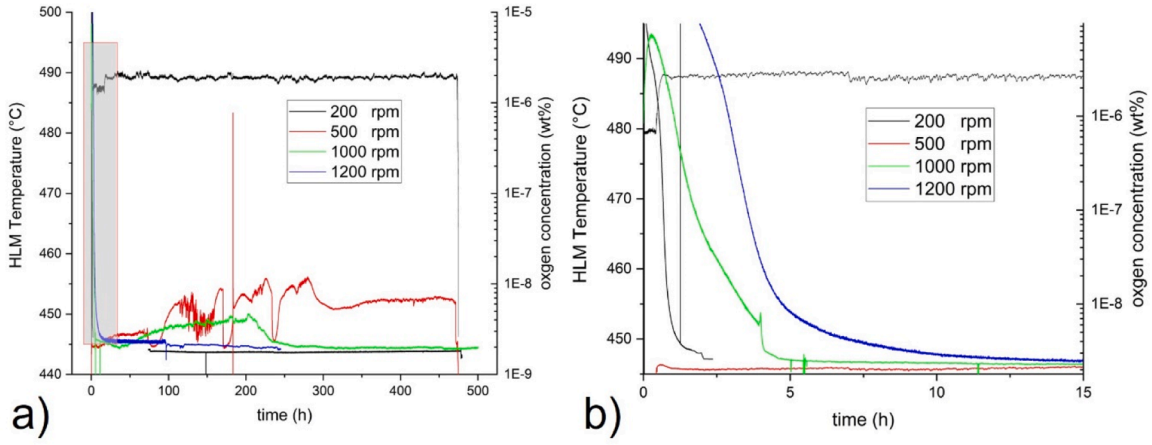

Fig. 6. a) Measured test temperature and oxygen concentration (wt.%) in the liquid PbBi during the entire test and b) in the first 15 h of the test.

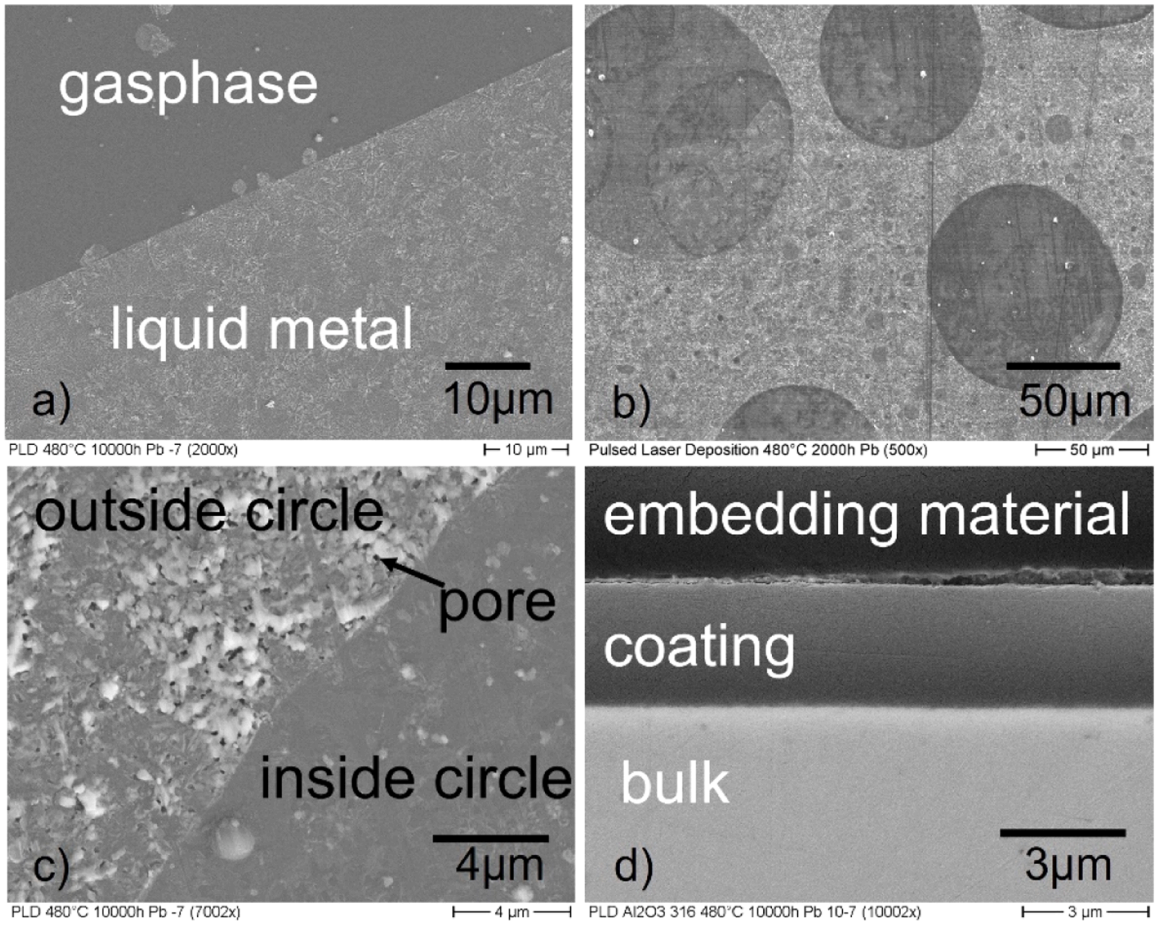

Fig. 7. SEM surface photos of the PLD sample after exposure to Pb with 10^{-7} wt.% oxygen at 480 °C; a) border between Pb exposed part and non-immersed part that was exposed to gas atmosphere (10,000 h sample); b) circle formation at the surface after 2000 h exposure in Pb; c) border between the inside (right side, dark grey) and the outside (left side, brighter area) of the circles (10,000 h sample); d) cross-section of PLD sample after 10,000 h exposure.

tuning the rotational speed of the inner cylinder. For the experiments presented here, rotation speeds of 200, 500, 1000, and 1200 rpm (rounds per minute) were used. According to numerical simulations that accompanied the experiments, the average speed along the lateral surfaces of the samples was between 0.3 and 1.6 m/s, see Table 3. This agrees with the expected flow velocity of 1.1 m/s in the core of ALFRED [29].

The flow conditions inside the CORELLA facility are described in detail elsewhere [31], but for a better understanding of the flow conditions a visualization of the flow field on an exemplary cross-section was depicted in Fig. 5c. In order to investigate the flow around the edges more closely, a high-resolution simulation of a uniform flow around one specimen with a flow velocity of 0.8 m/s was performed, Fig. 5d. The specimen was tilted by 2 degrees against the flow to mimic

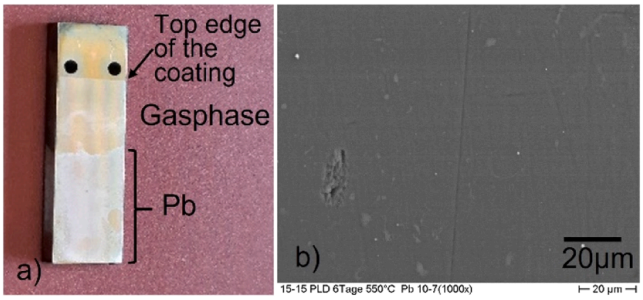

Fig. 8. a) Photo of the PLD sample after 144 h exposure to Pb at 550 °C; b) surface of the part exposed to the gas phase showing a smooth surface with some small defects known from the non-exposed sample (SEM photo).

the slightly tilted attack on the leading edges (facing the flow) of the specimens in the exposure chamber. Directly at the specimen surface, the fluid velocity decreases to zero due to the no-slip boundary condition. The maximum speed, which is increased by 36 % compared with the uniform flow, is obtained at the edges of the leading edge. Obvious is that recirculation zones are formed on both lateral surfaces directly after the leading edge and at the trailing edge (rear edge). Reattachment of the flow occurs on the lateral surfaces, where the position of reattachment depends on the tilt of the specimen against the flow. Such turbulent flows can also occur inside a nuclear facility for example inside the core due to spacer grids or at a wire-wrapped fuel assembly as foreseen in MYRRHA.

The measured temperature and oxygen concentration in the liquid PbBi during the test are depicted in Fig. 6. The temperature was around 480 °C in the first hour, cf. Fig. 6b, increased then to around 490 °C and remained there for the rest of the test, cf. Fig. 6a. It was planned to conduct the tests with an oxygen content of 10^{-6} wt.% in the PbBi, which is one of the targeted oxygen concentrations in a Pb/PbBi cooled nuclear installation. Therefore, in the conditioning chamber the liquid metal was preconditioned to the envisaged oxygen concentration and then transferred to the test chamber. Inside the test chamber the oxygen content was measured at the bottom in a region with low flow velocity with an oxygen sensor with a Bi/Bi_2O_3 reference electrode. With the exception of the test at 500 rpm, the oxygen concentration in the liquid metal was above 10^{-6} wt.% at the beginning, decreased within 6 h to values below 10^{-8} wt.%, and remained at around 2×10^{-9} wt.% for the rest of the exposure. In case of the 500 rpm test, the oxygen content decreased in the first hour very quickly to 2×10^{-9} wt.% and fluctuated for the rest of the experiment around 7×10^{-9} wt.%. Although the oxygen partial pressure in the gaseous phase above the liquid metal was increased above the saturation concentration of oxygen in PbBi, it was not possible to reach a higher oxygen content at the bottom of the test chamber. It should be noted that in addition to the alumina coated samples also austenitic steel samples without coating were exposed in the same experiment, which revealed solution attack and erosion. It seems that the oxygen consumption due to the presence of these samples could not be compensated by the oxygen transfer from the gaseous phase to the liquid metal across the gas/PbBi interface and/or the oxygen transport inside the liquid metal.

The exposure time was 480 h for the experiments with 200, 500, and 1200 rpm and 500 h for the experiment with 1000 rpm.

2.4. Post exposure analysis

After the exposure experiments, the samples were cleaned from the adherent Pb/PbBi residual crusts for 30 min with a 1:1:1 solution of deionized water, hydrogen peroxide (30 %), and acetic acid (96 %) in order to expose the coating surface and allow for its characterisation. The pack cementation and DG samples exposed for 2000 and 6528 h at 480 °C received a Ni plating after exposure to the liquid metal to avoid a rounding of the sample edges during cross-section preparation. This was omitted for the other samples. Afterwards, samples were embedded without cutting to avoid a spalling of the coating, grinded and polished down to a 1 µm diamond paste. Both specimen surface and cross-section of the specimens were investigated by using a light optical microscope (LOM—Olympus BX60M), scanning electron microscopes (SEM—Hitachi S-4800 with cold field emission electron source and Zeiss

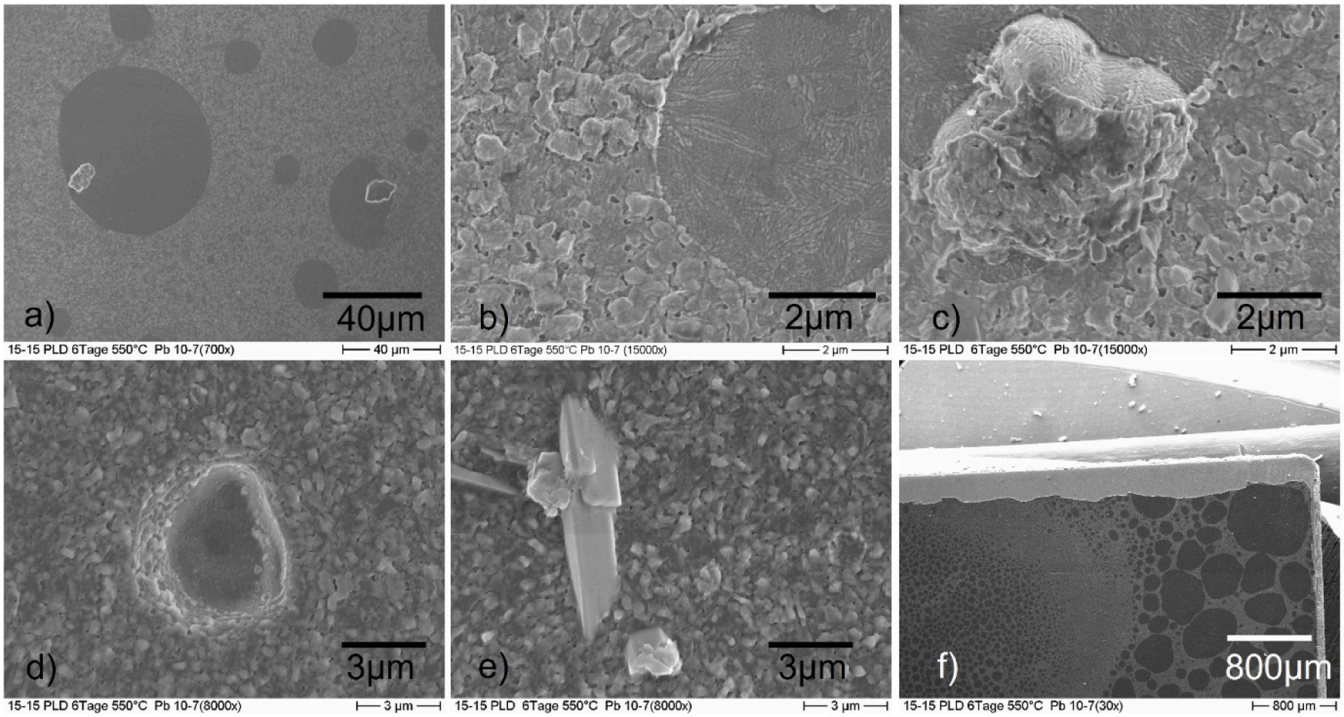

Fig. 9. SEM photos of the PLD sample surface exposed at 550 °C to Pb with 10^{-7} wt.% oxygen for 144 h; a) and b) circular areas and grain growth, c) and d) defects, e) larger grains with a higher Pb concentration, and f) chipping of the coating at the edge.

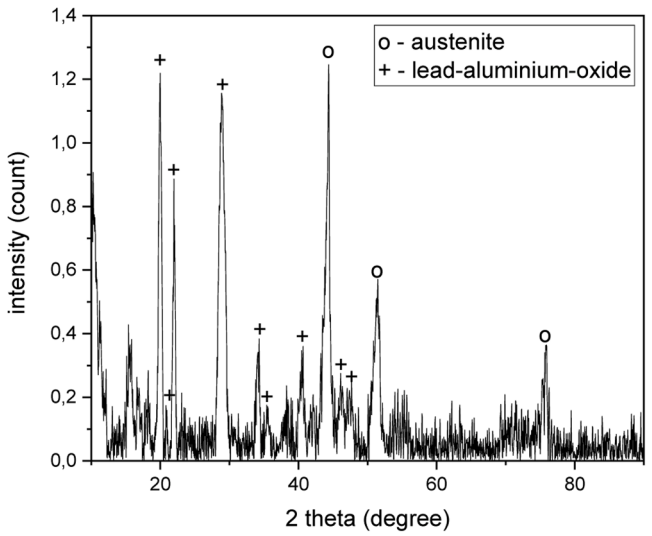

Fig. 10. GIXRD pattern of the PLD sample surface exposed at 550 °C to Pb with 10^{-7} wt.% oxygen for 144 h.

LEO 1530 VP with a Schottky-field emission gun) with integrated energy dispersive X-ray spectroscope (EDS), and a x-ray diffractometer (XRD - Seifert PAF II with Cu- Kα1 radiation ($\lambda = 0.15406$ nm, 40 kV and 30 mA)).

3. Results

The result chapter is split in two parts. In the first part, results of the corrosion test conducted in the COSTA facility with stagnant Pb are presented, while the second part deals with the results of the CORELLA experiments with flowing PbBi.

3.1. Corrosion tests in stagnant Pb (COSTA facility)

3.1.1. PLD coatings

The PLD coating protected the surface of the steel during the entire 10,000 h exposure at 480 °C in Pb with 10^{-7} wt.% oxygen, although the parts that were immersed in Pb lost the original mirror finishing, looking matte. Fig. 7a shows the transition between the gas atmosphere and the immersed part. A slight change in the structure of the surface exposed in the liquid metal is noticeable. The surface that was in contact with the gas atmosphere appears dark and smooth, while that one exposed to Pb appears bright. In contact with the liquid metal, grain growth starts with the formation of pores and Pb inclusions. Additionally, circular areas with a slower grain growth likely due to non-uniform wetting are visible as in Fig. 7b. Fig. 7c shows the border between a circle (dark part) and the brighter part outside the circle. The bright parts show Pb enrichments with up to 36 wt.% measured by EDS and the dark spots are the above-mentioned pores. In the cross-section, this is not noticeable even after 10,000 h, see Fig. 7d, indicating that it is only a moderate reaction at the very outer surface. This change was also not detectable by a conventional θ/2θ analysis. The XRD pattern of the sample surface shows only the peaks from the bulk material (austenite), because the

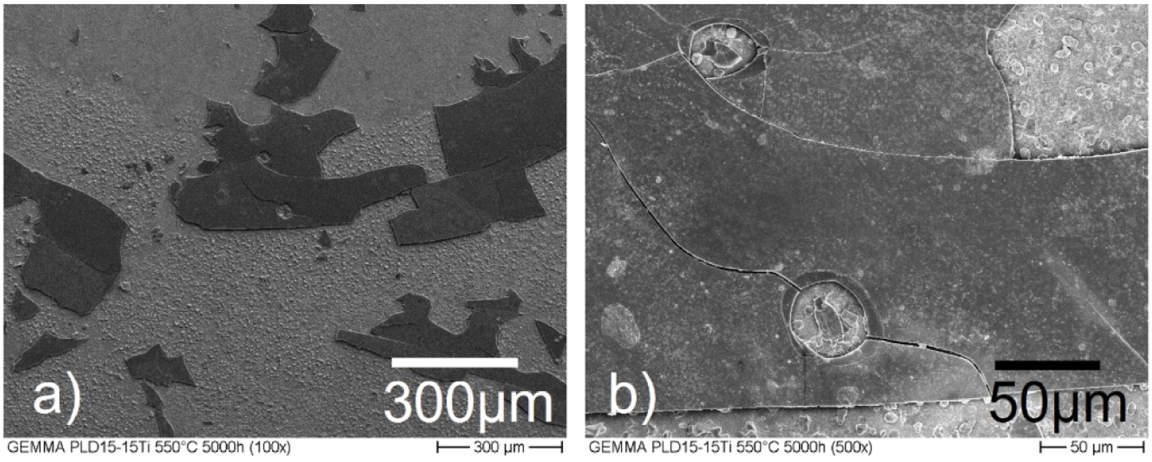

Fig. 11. SEM photos of the PLD sample surface after 5000 h exposure at 550 °C to Pb with 10^{-7} wt.% oxygen showing a) severe exfoliation of the coating and b) remains of the coating with cracks and circular defects.

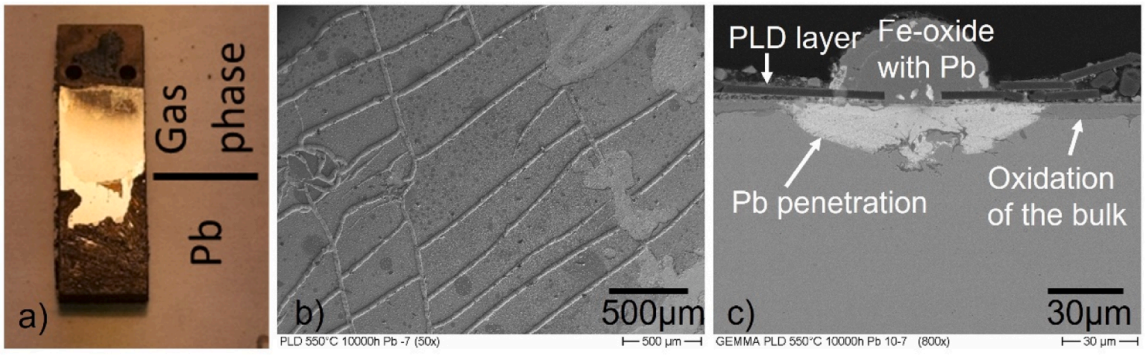

Fig. 12. Photo and SEM pictures of PLD sample after 10,000 h at 550 °C in Pb with 10^{-7} wt.% oxygen, a) sample after cleaning; b) field like pattern due to cracks in the coating; c) cross-section through an elevation in the field pattern.

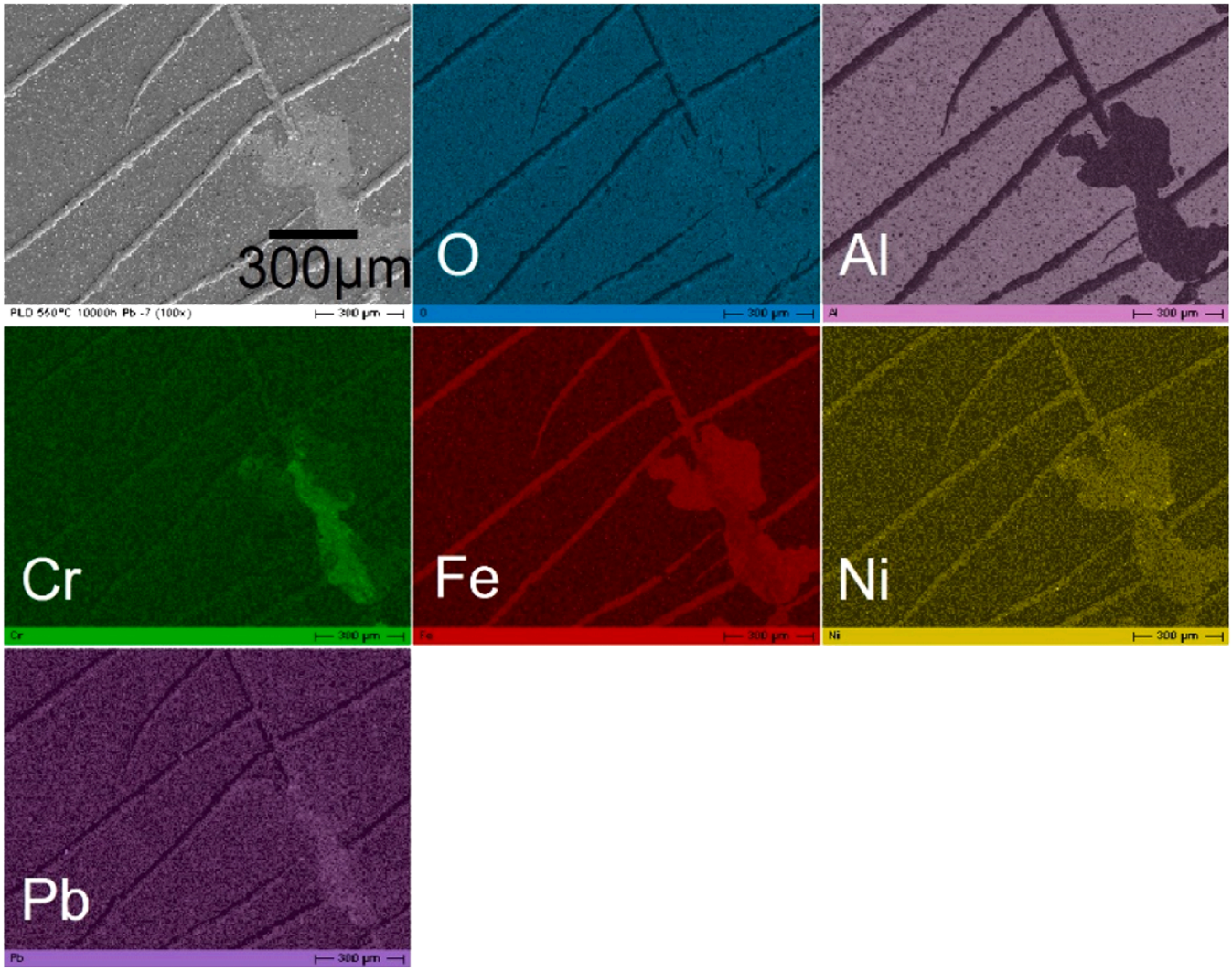

Fig. 13. Elemental mapping images of the PLD sample after 10,000 h exposure at 550 °C in Pb with 10^{-7} wt.% oxygen.

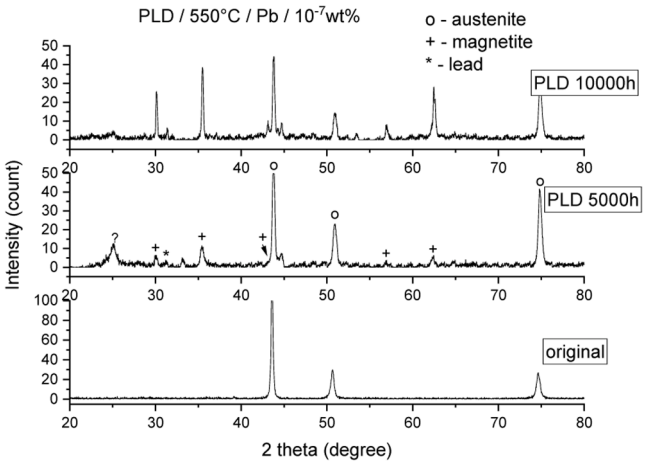

Fig. 14. X-ray diffraction pattern of the sample surface after 5000 h and 10,000 h at 550 °C in Pb with 10^{-7} wt.% oxygen and of the pristine sample (original).

coating is amorphous and very thin.

At 550 °C after 144 h exposure, the behaviour of the PLD coating is similar with that at 480 °C. The surface part that was exposed to the gas atmosphere is still shiny and smooth with some small defects known from the non-exposed surface, see Fig. 8a, b. In contrast, the part that was exposed in Pb is white tarnished, Fig. 8a. Surface examinations with a higher magnification exhibit grain growth with the formation of pores, Pb enrichments and circular areas as shown in Fig. 9a, b. Additionally, many defects are visible on the surface (Fig. 9c, d) and some larger grains appear with a high concentration of lead (68–82 wt.%) and small amounts of O, Al, and Fe (Fig. 9e). Noticeable is the chipping of the coating at the edges (Fig. 9f), which can be observed on the whole sample independently of the exposure medium (lead–gas atmosphere).

Due to the large penetration depth of a conventional θ/2θ analysis it is not possible to provide information about the grains formed at the surface. Therefore, a grazing incidence X-Ray diffraction (GIXRD) measurement with a fixed incidence angle of 2° was performed. It clearly shows that a reaction took place between the PLD coating and the liquid Pb on the surface resulting in the formation of $Pb(Al_2O_4)$ (ICDD 01-83-1016), see Fig. 10. Additional peaks from the base material, 15-15Ti steel, can be seen as well in the GIXRD pattern.

After 5000 h and 10,000 h at 550 °C, the coatings showed severe exfoliation as depicted in Figs. 11 and 12. No shiny surface is visible on the 5000 h exposed sample in Pb and indeed, the dark parts in the SEM micrograph in Fig. 11a are the remains of the initial PLD coating. All other brighter areas are oxidized bulk material; Cr, Fe, Ni and O are detected by EDS analysis. Fig. 11b shows better the remains of the PLD coating featuring cracks and circular defects.

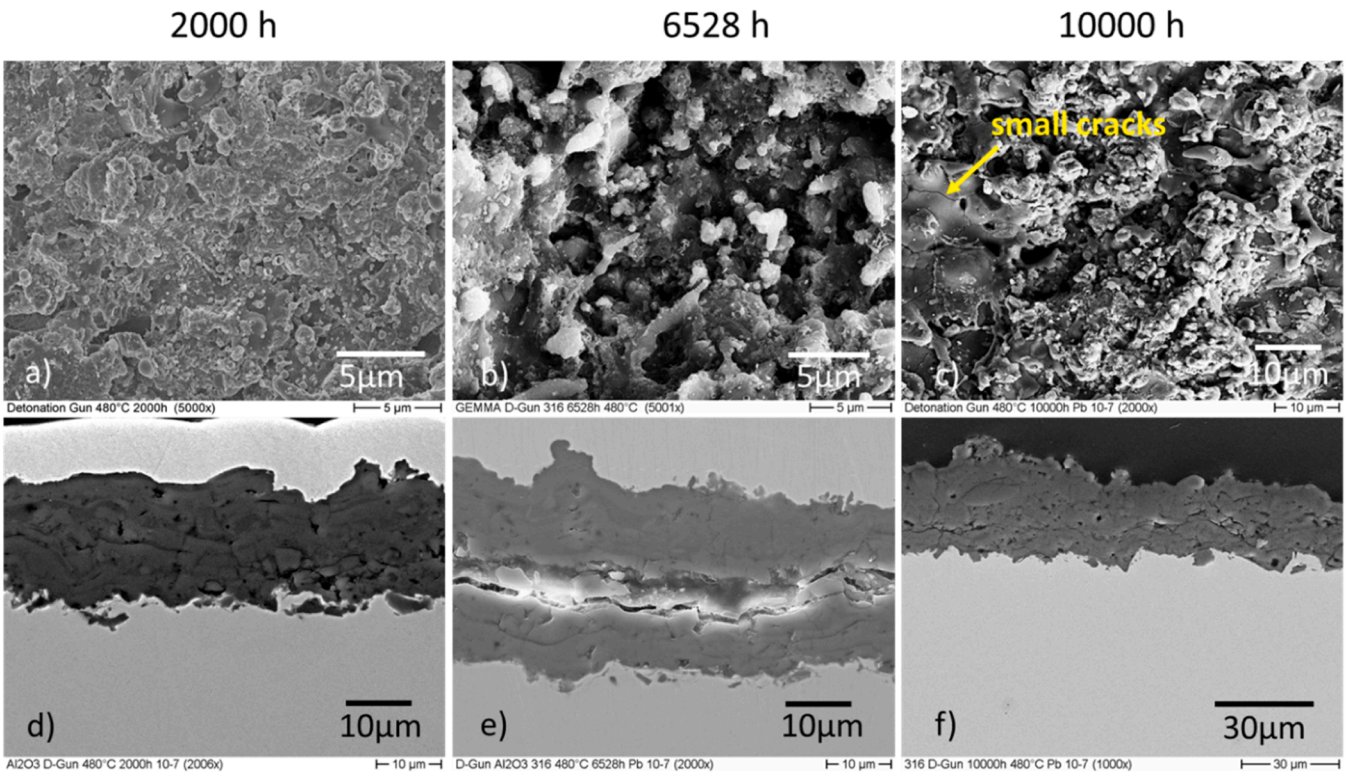

Fig. 15. SEM photos of the surface (a, b, c) and cross-section (d, e, f) of the DG samples after 2000 h, 6528 h, and 10,000 h exposure at 480 °C in Pb with 10^{-7} wt. % oxygen.

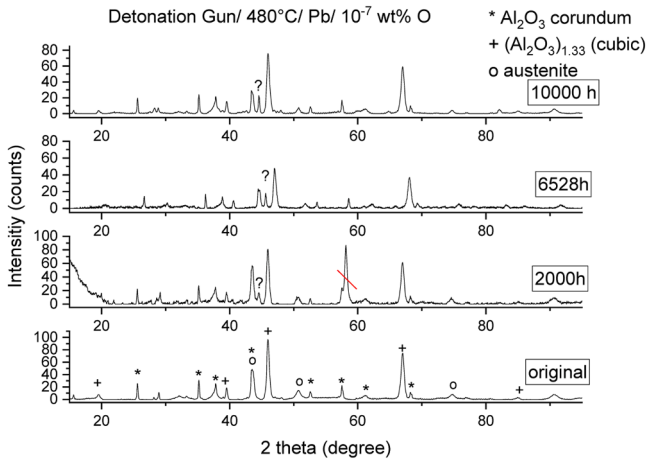

Fig. 16. X-ray diffraction pattern of the sample surface after 2000 h, 6528 h, and 10,000 h at 480 °C in Pb with 10^{-7} wt.% oxygen and of the pristine sample (original); the crossed-out peak in the measurement of the 2000 h sample is a mis-measurement of the XRD instrument due to scattered radiation.

In the case of the 10,000 h exposed sample, a remaining part of the shiny coating was visible mainly in the area exposed to the gas phase, as shown in Fig. 12a. The rest of the sample shows severe exfoliation of the coating. Part of the exfoliation is similar to that observed after 5000 h, cf. Fig. 11, but also field-like patterns separated by lines occur in regions where the alumina coating is still attached, as in Fig. 12b. An EDS elemental mapping of such an area is displayed in Fig. 13, showing that the crack lines consist mainly of iron oxide with low amounts of Ni and Cr. When cracks occur, oxygen can react with the bulk surface forming iron oxide that grows outwards. Furthermore, liquid Pb can penetrate through these cracks into the bulk, as demonstrated in Fig. 12c. Fe-oxide crystals are also visible on the remaining coating. Beside these crack lines, circular defects also appear, similar to those shown at the 5000 h exposed sample (cf. Fig. 11b).

In order to strengthen these observations, X-ray diffraction patterns were recorded on the sample surfaces after 5000 h and 10,000 h exposures, confirming the results of the EDS analysis. The diffractograms reveal austenite peaks coming from the bulk material and magnetite peaks because of the bulk material oxidation as shown in Fig. 14.

3.1.2. *Detonation gun (DG)*

SEM images of the DG samples after 2000 h, 6528 h, and 10,000 h exposure at 480 °C in liquid Pb with an oxygen content of 10^{-7} wt.% are shown in Fig. 15. Neither a detachment nor a structural change of the DG alumina coating is visible. In general, DG coatings are characterised by the rough morphology visible in the micrographs, which does not affect the corrosion protection capability. The same applies for the small cracks (Fig. 15c) visible on all the surfaces. Those cracks are typical features of DG coatings due to abrupt cooling of the molten alumina droplets during deposition, which solidify shrinking on the cold substrate surface. The large crack in the coating after 6528 h as shown in Fig. 15e occurred most probably due to a too thick Ni plating applied during SEM samples preparation.

X-ray diffraction patterns of the sample surfaces are depicted in Fig. 16. At the bottom, the pattern of the original non-exposed sample is presented. It consists of two different Al_2O_3 crystalline phases, a thermodynamically stable rhombohedral α-Al_2O_3 phase called corundum and a metastable cubic structure (γ-Al_2O_3). These phases remain over the entire exposure time, but an additional peak appears at 44.68 degrees. It is marked with a question mark, because a final identification was not possible. From the available database, only the reference pattern of hexagonal Al_2O_3 (JCDD 10-414) has a peak at this angle. Furthermore, peaks from the underlying steel are detected due to the high penetration depth of the X-rays in Al_2O_3.

Similar to the samples exposed at 480 °C, no changes are observed in

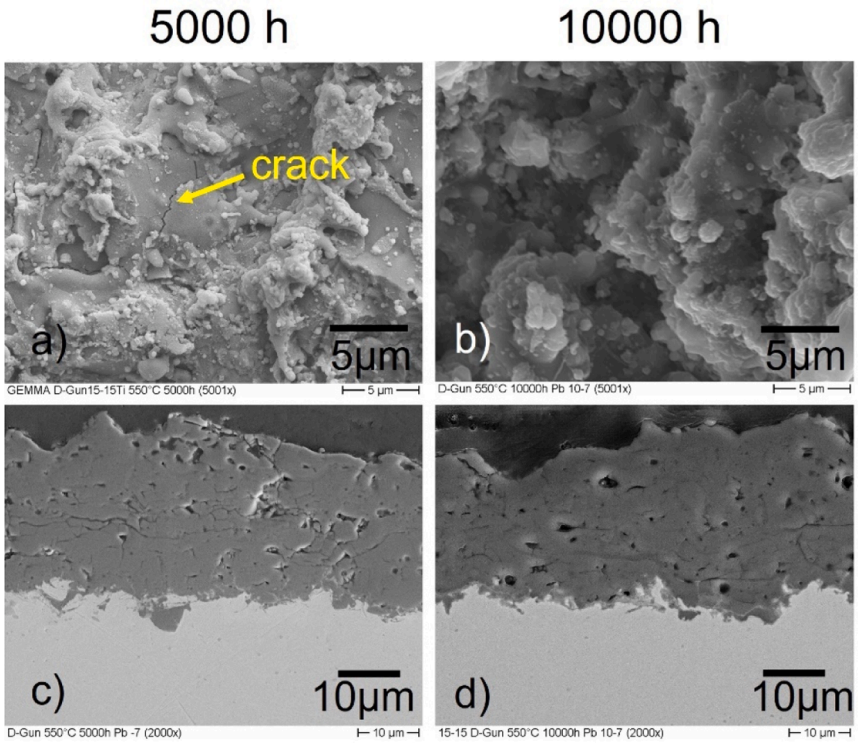

Fig. 17. SEM photos of the surface (a, b) and cross-section (c, d) of the DG samples after 5000 h and 10,000 h exposure at 550 °C in Pb with 10^{-7} wt.% oxygen.

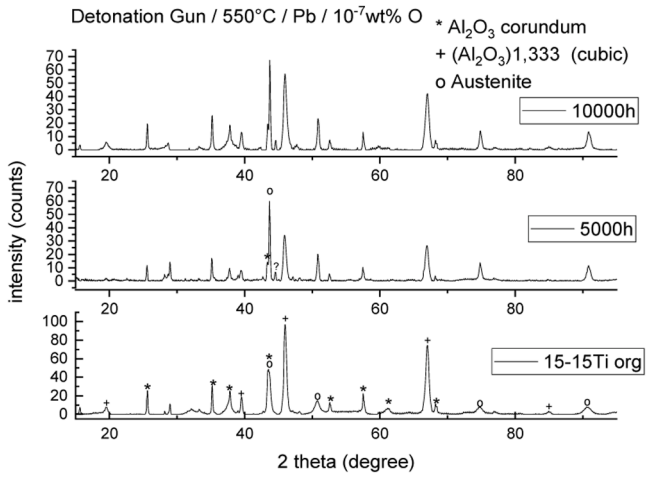

Fig. 18. X-ray diffraction pattern of the sample surface after 5000 h and 10,000 h at 550 °C in Pb with 10^{-7} wt.% oxygen and of the as-delivered sample (original).

the coating exposed at 550 °C after 5000 h and 10,000 h (see Fig. 17). The coating remains adherent to the steel substrate and no delamination is observed. Also in these samples, the small cracks typical of the DG coatings are visible at the surface as on the samples exposed at 480 °C, which do not seem to have a negative impact on the protective behaviour of the coating.

The X-ray diffraction pattern of these coating samples are shown in Fig. 18. All of the three patterns show peaks coming from Al_2O_3 with different crystalline phases (mainly α- and γ-Al_2O_3) and from the 15-15Ti substrate steel. At around 43.5 degree, the main peak from 15 to 15Ti is partially superimposed by the α-Al_2O_3 peak. Note that in the pattern of the original sample this peak is wider while it gets separated over time (at 5000 h and 10,000 h), probably because the materials' crystallites grew after the heat received and the XRD peaks became sharper and more resolved or because of a phase transition from γ-Al_2O_3 to α-Al_2O_3. Such a phase transition to a denser structure can lead to a volume change, which can cause cracks. Another possibility of the wider peak observed at the original pattern could be a deformation of the base material surface during the coating procedure by the impact of the coating material. During the exposure the material relaxes and the peak becomes sharp again. Like in the 480 °C pattern the peak at 44.68 degree appears, which may belong to a hexagonal Al_2O_3 (JCDD 10-414).

3.1.3. Pack cementation

Images of the pack cementation sample surface after exposure at 480 °C are depicted in Fig. 19. Obvious is the formation of flake-shaped crystals at the surface over time, visible well at the SEM photo Fig. 19c after 10,000 h exposure. On the cross-section images, the typical Al diffusion layer is visible as in Fig. 19f. Already at the as-delivered sample an oxygen enrichment was measurable at the surface and at the interface to the Al diffusion layer indicating formation of alumina at the surface. This layer is maintained or proceed to grow during exposure. No corrosion attack by liquid Pb was observed at any of the pack cementation samples.

XRD patterns of the surfaces of the samples are depicted in Fig. 20. The peaks can be assigned to NiAl. No alumina peak is detectable, because the alumina scale is too thin.

3.2. Corrosion tests in turbulently flowing PbBi (CORELLA facility)

3.2.1. Pulsed laser deposition

The shiny surfaces of the pristine PLD samples became matte in some areas after the tests with 200 rpm (0.3 m/s) and 500 rpm (0.8 m/s) at 490 °C and an exposure time of 480 h as shown in Fig. 21. EDS measurements of the matte surface show that Pb (potentially oxidized) with low amounts of Fe and Cr covers these surfaces. The 1000 rpm (1.4 m/s / 500 h) sample conserved the shiny surface during the test, while the sample exposed at 1200 rpm (1.6 m/s) has a black surface appearance. On the 1200 rpm sample there are deposits of Cr-oxide with small

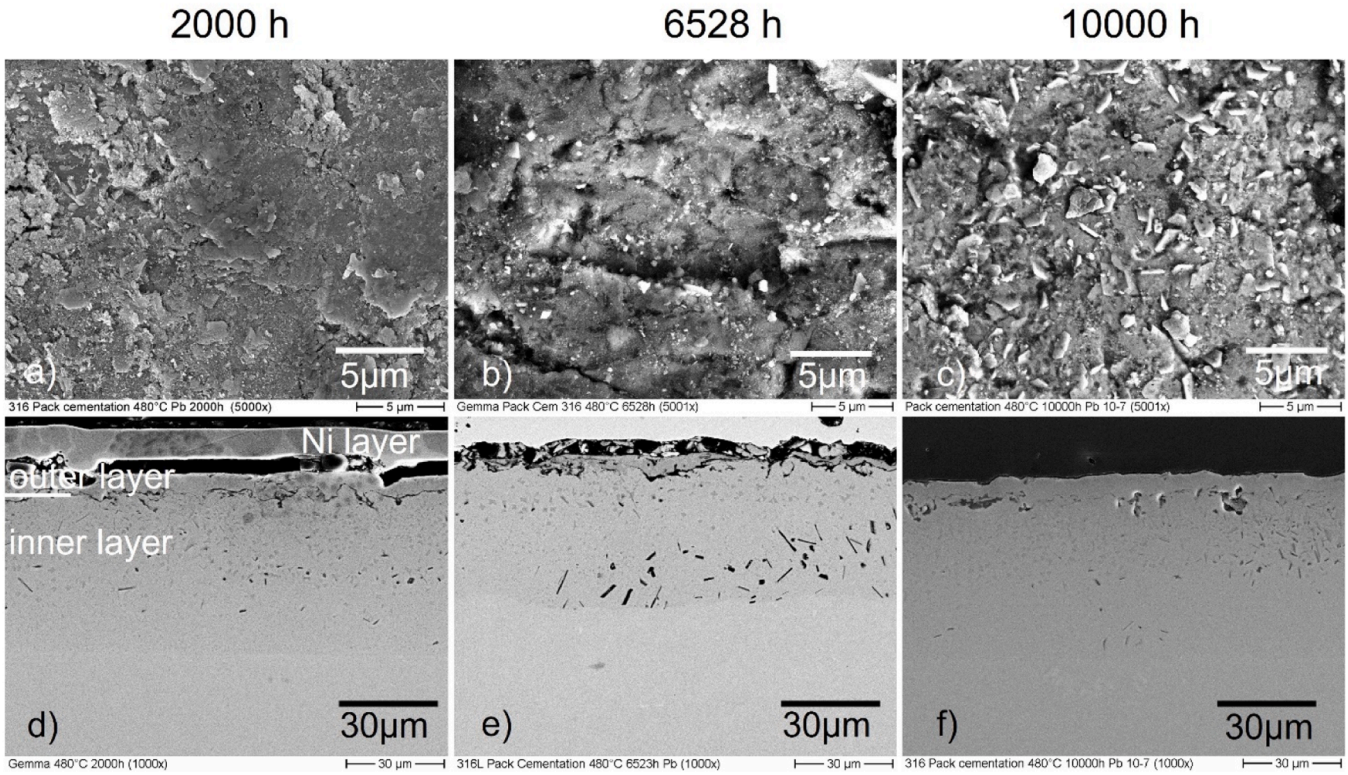

Fig. 19. SEM photos of the surface (a, b, c) and cross-section (d, e, f) of the pack cementation samples after 2000 h, 6528 h, and 10,000 h exposure at 480 °C in Pb with 10^{-7} wt.% oxygen.

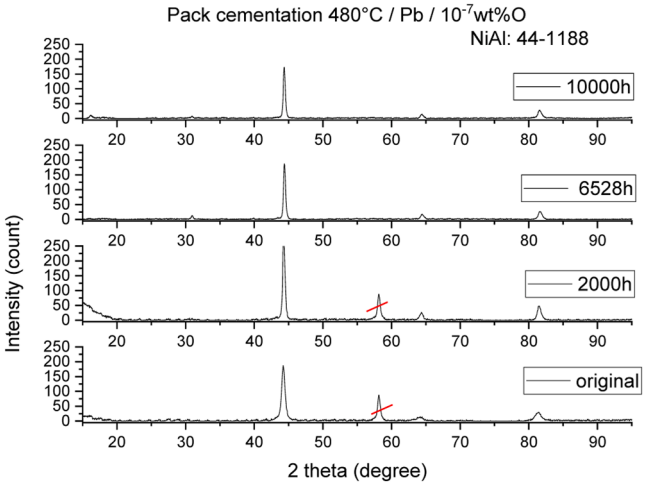

Fig. 20. X-ray diffraction pattern of the sample surface after 2000 h, 6528 h, and 10,000 h at 480 °C in Pb with 10^{-7} wt.% oxygen and of the as-delivered sample (original); the crossed-out peak in the measurement of the original and the 2000 h sample is a mis-measurement of the XRD device due to scattered radiation, the other peaks can be assigned to NiAl.

amounts of Fe and Pb, which are oxidized solute products from other exposed samples.

Apart from these deposits, neither changes in the coatings or in the underlying material are visible after exposure, nor is any detachment of the alumina coating observed in the cross-sections as shown in Fig. 22. The PLD coatings protect the steels under these conditions.

In addition to the lateral flat surface of the samples, either the trailing edge (200, 500, and 1000 rpm) or the leading edge (1200 rpm) is coated by alumina, although much thinner. Even the very thin coating on the edges protects the steel from any influence by the turbulently flowing PbBi, see Fig. 23. In particular, no spallation of the coating is observed, not even along the edges with the harshest flow conditions. One exception is the corner at the trailing edge of the sample exposed at 500 rpm, see Fig. 23f. Here, a defect led to a dissolution attack (depletion in Ni and Cr) and inclusion of Pb and oxygen. This behaviour is similar to the non-coated edges. The non-coated edges show erosion-enhanced corrosion at all speeds. The base material was 316L in the experiments at 200, 500, and 1000 rpm, and 15-15Ti for 1200 rpm.

3.2.2. *Detonation gun*

The DG samples show neither change or detachment of the alumina coating after exposure nor any change of the steel underneath, see Fig. 24. The only effect noticed is a thin layer of deposits observed on the surface of the coatings exposed at 500, 1000, and 1200 rpm. These deposits consist mainly of Fe-Cr oxides, oxidized solute products from

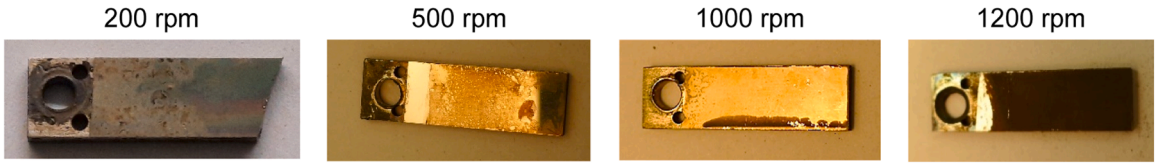

Fig. 21. Photos of the PLD samples after exposure.

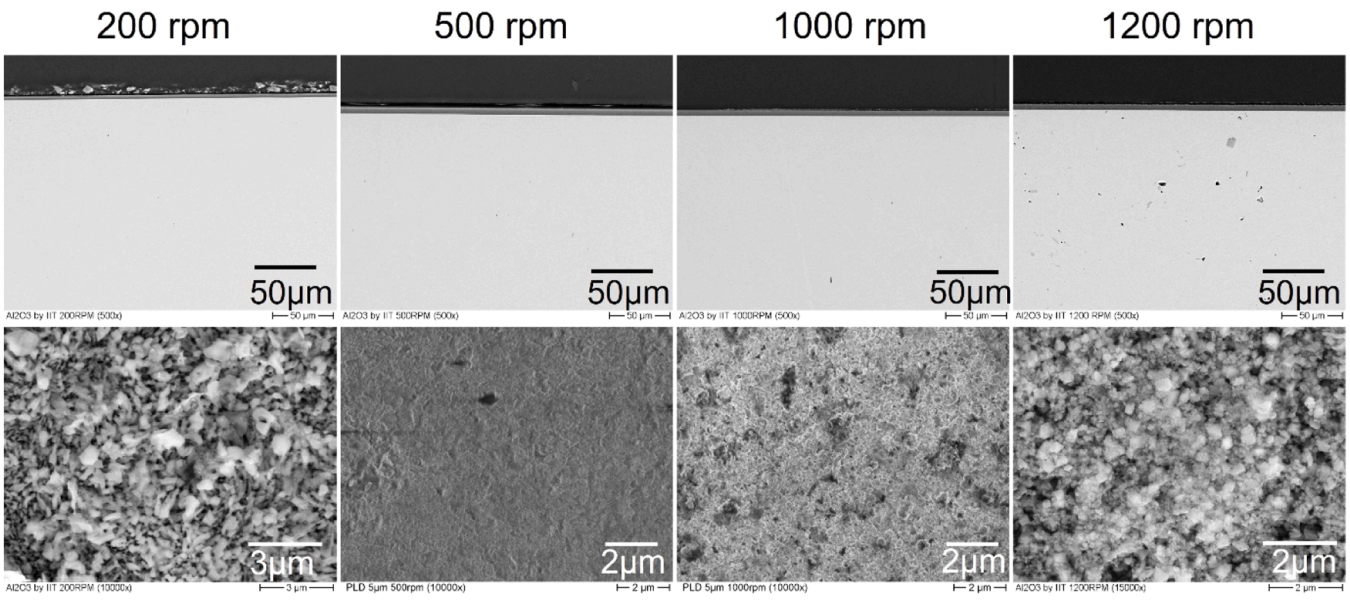

Fig. 22. SEM images of the surface (upper row) and the cross-section (lower row) of PLD samples after exposure to different flow velocities.

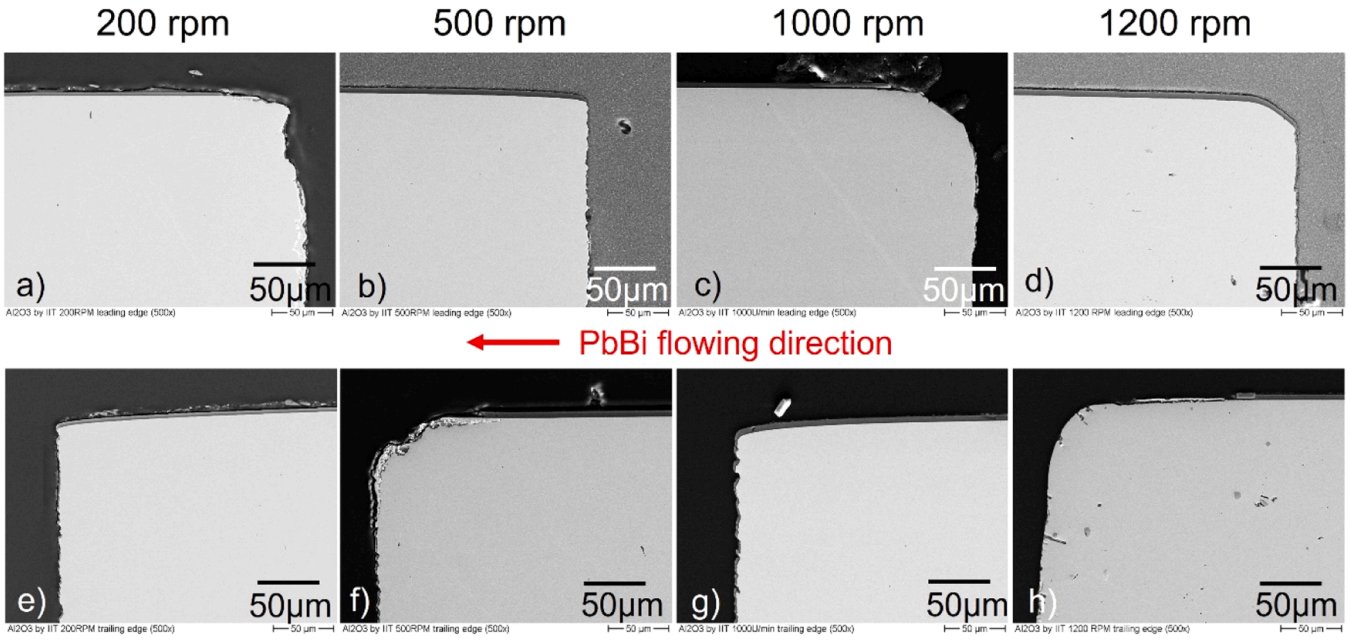

Fig. 23. Cross-section SEM photos of leading (a–d) and trailing (e–h) edges of the PLD alumina coated samples after exposure at different speeds.

other exposed samples, with small amounts of Pb similar to the 1200 rpm PLD sample. In the light of these data, it can be concluded that the alumina coatings produced by detonation gun successfully protect the steel substrate material from corrosion/erosion attack at these conditions.

The analysis of the XRD pattern shows that the coating consists of different Al_2O_3 crystalline phases (rhombohedral α-Al_2O_3 and metastable cubic (γ-) structure), as in the static exposure experiments. A peak at 44.68 degrees becomes visible, which most likely belongs to the hexagonal Al_2O_3 phase (JCCD 10-414). Any additional effect due to the highly turbulent flow field of PbBi could not be detected.

The samples coated with alumina by detonation gun on the flat surface did not show the same high-quality coating on the edges, because the deposition protocol used does not aim for optimal coverage of edges, but only of flat surfaces. Indeed, the layer at the edge is much thinner or even missing as shown in Fig. 2. Accordingly, the leading and trailing edges of the samples after exposure, see Fig. 25, show inclusions of Pb (see, e.g., leading edge at 500 rpm (Fig. 25b), localized erosion/non-selective leaching (leading edges at 1000 and 1200 rpm, Fig. 25c-d), and dissolution (selective leaching) attack (trailing edge at 1200 rpm, Fig. 25h). Note that the base material was 316L for the samples exposed at 200 and 500 rpm and 15-15Ti for the experiments at 1000 and 1200 rpm.

4. Discussion

Three different alumina / alumina-forming coatings were tested in liquid Pb with 10^{-7} wt.% oxygen at 480 °C and 550 °C up to 10,000 h. For the alumina coating two different deposition methods were applied: pulsed laser deposition and detonation gun. At a temperature of 480 °C,

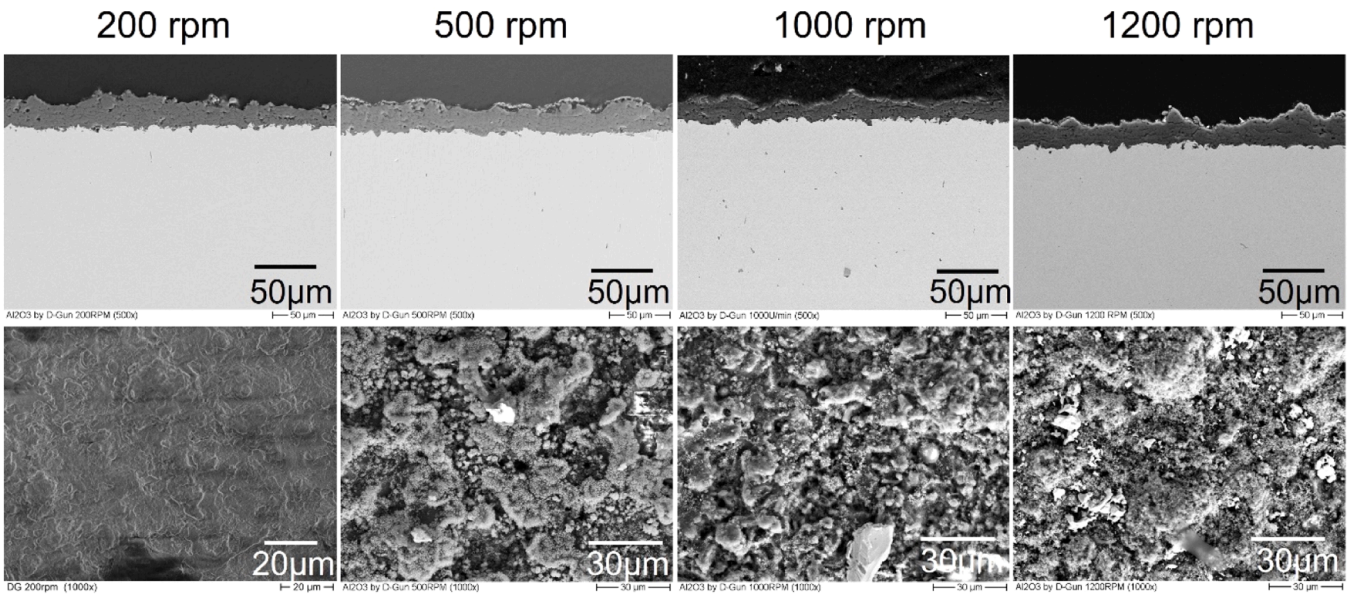

Fig. 24. SEM photos of the surface (upper row) and the cross-section (lower row) of DG samples after exposure to different flow velocities.

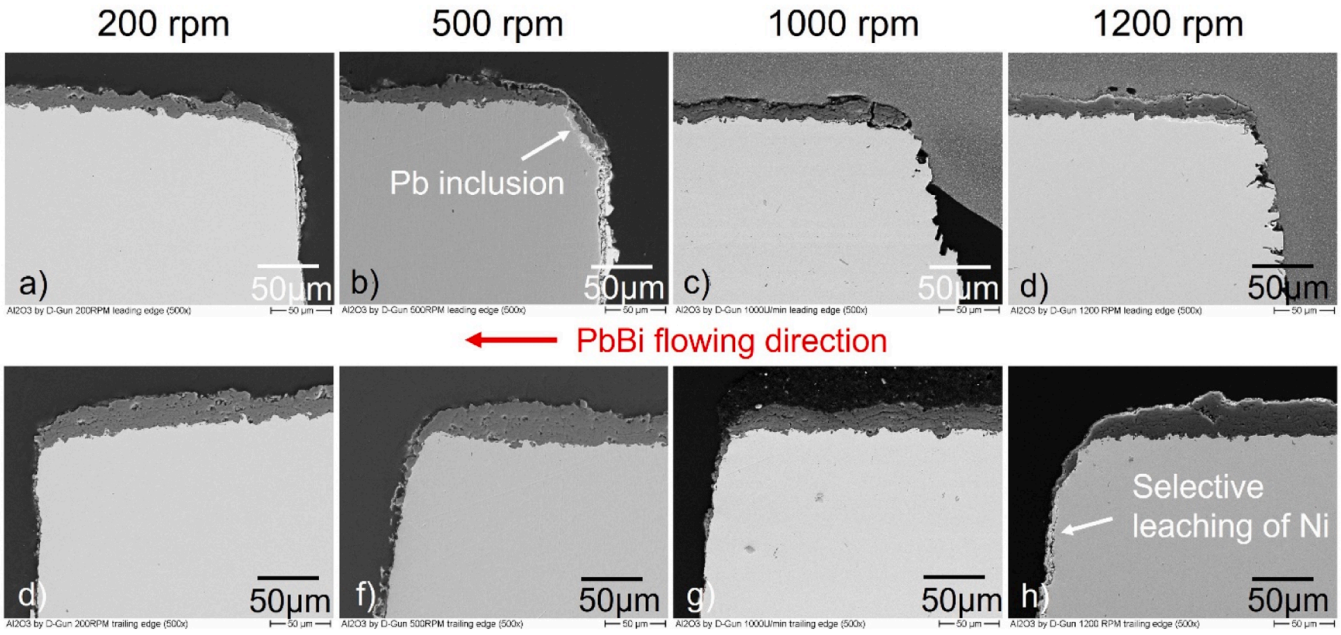

Fig. 25. Secondary electrons SEM micrographs showing the cross-section structure of the leading (a–d) and the trailing (d–h) edges of the DG samples after exposure at different speeds.

the PLD sample showed no corrosion up to 10,000 h but a slight reaction with Pb at the surface, which was also described in Ref. [12]. At the higher temperature of 550 °C and after a short exposure time of 144 h this slight reaction was also observed. A GIXRD measurement clearly identified the formation of $Pb(Al_2O_4)$. The PLD coating has a mainly amorphous Al_2O_3 matrix [7]. An amorphous matrix is thermodynamically less stable compared with a crystalline one. Crystalline Al_2O_3 is known to be compatible with liquid Pb at these conditions [32]. This might be the reason for the observed reaction with lead. The reaction layer is still very thin after 10,000 h exposure, which does not allow any statement about potential growth of the layer as a function of time and temperature. However, the formation seems to be oxygen dependent, because this reaction was not detectable on the samples exposed to turbulently flowing LBE. The oxygen content there was close to 10^{-6} wt. % only in the first hours and then dropped to 2×10^{-9}–7×10^{-9} wt.%. Overall, this $Pb(Al_2O_4)$ layer seems to have no negative impact on the protection capability of the PLD coating at the temperature and time tested.

Additionally, spalling of the coating at the edge was observed on the sample exposed at 550 °C for short time, which can cause the coating to fail at longer exposure times. The coating exhibited cracks and delamination at higher temperature exposure. The underlying steel substrates started to oxidize and dissolution attacks occurred. These results are in contrast to the exposure data reported in Refs. [8,9], where neither delamination or cracks nor oxidation of the substrate material was observed. A possible explanation for this could be an edge effect that occurs at higher temperatures, because the coating was only applied on one side and the slightly bevelled edges have an insufficient coating.

Another reason could be the imperfection during the coating process (e.g., large droplets); a preferential oxidation of the substrate will start there. Such localized oxidation can spread also beneath the coating, result in stress, and can foster the delamination of the coating. At 550 °C, such an effect is significantly more pronounced than at 480 °C. To further investigate these effects, long-term tests should be repeated at 550 °C with a fully coated defect-free PLD sample. In this context, the influence of the Pb(Al_2O_3) on the coating can be analysed in more detail to analyse the potential influence of the crystallisation of the aluminate on the cracking.

In the corrosion experiments in turbulent LBE flow, the temperatures were comparable to those in stagnant Pb at 480 °C. The PLD coating showed very good behaviour in flowing conditions up to 1.6 m/s with an oxygen content below 10^{-8} wt.%; no change in the coating and no detachment was observed. Moreover, the much thinner coating on the trailing edge (200, 500, and 1000 rpm) or the leading edge (1200 rpm) is able to protect the steel, despite the increased turbulence at these locations.

As for the DG alumina coatings, all samples showed a good behaviour at all temperatures in stagnant Pb and flowing LBE. Neither spallation nor dissolution attack were observed and it was found that the high roughness of the coating has no negative impact on its corrosion protection properties. However, the coating is in a metastable condition. Although no considerable change in the crystalline structure measurable by XRD is observed at 480 °C in stagnant Pb and at 490 °C in flowing LBE, a transition from γ-Al_2O_3 to α-Al_2O_3 appears at 550 °C as well as an increasing crystallinity of α-Al_2O_3. The presence of the γ-Al_2O_3 and small amounts of other metastable Al_2O_3 in DG coatings is often reported in literature [13,14,33,34] and cannot be prevented, while their volume fraction strongly depends on the spraying mode [34]. An increase of the volume fraction of α-Al_2O_3 can also be beneficial to the mechanical properties; it increases the wear resistance and hardness [33]. In any case, DG alumina coatings demonstrated to resist the corrosion independently of the phase structure owned.

The alumina-forming coating produced by pack cementation was tested only at 480 °C in stagnant Pb. For this kind of coating, no signs of corrosion are noticed up to 10,000 h of exposure in the liquid metal. This coating develops a very thin and protective alumina layer and some flake-shaped crystals are growing on the surface over time. After oxidation tests in air, needle and platelet crystals were observed on the surface of aluminide diffusion coatings produced by pack cementation at temperatures below 1000 °C [35]. Similar needles were observed at these temperatures on alumina-forming ODS (oxide dispersion strengthened) superalloys [36]. In both cases it was θ-Al_2O_3, which is known to be formed below 1000 °C. It can therefore be assumed that θ-Al_2O_3 was also formed during exposure in the current study.

5. Conclusions

Two alumina coatings (produced by pulsed laser deposition (PLD) and detonation gun (DG)) and one alumina-forming coating produced by pack cementation were tested in oxygen-controlled stagnant Pb (10^{-7} wt.%) at 480 °C and 550 °C up to 10,000 h and in turbulently flowing (up to 1.6 m/s) PbBi at 490 °C with 10^{-9}–10^{-8} wt.% oxygen for about 500 h.

Based on the results following conclusions could be drawn:

- Alumina coatings produced by pulsed layer deposition (PLD) protect steels at around 480 °C in stagnant Pb with 10^{-7} wt.% oxygen and in flowing PbBi with oxygen concentrations in the range 10^{-9}–10^{-8} wt.% and a flow velocity up to 1.6 m/s. Even the much thinner coating on the trailing or leading edges is able to protect the steel against erosion-corrosion.
- At 550 °C, probably because the coating was discontinuous, the PLD coating chipped at the edges even after short exposure times, which lead to severe exfoliation and a corrosion attack of the steel.
- Alumina coatings produced by detonation gun show a good behaviour at all temperatures in stagnant Pb and flowing PbBi. Neither delamination nor signs of dissolution are visible on the samples. The small cracks observed at the surface, which are typical features of this type of coatings, do not seem to have a negative impact on the corrosion protection capabilities.
- Alumina-forming coatings produced by pack cementation were tested only at 480 °C in stagnant Pb with 10^{-7} wt.% oxygen up to 10,000 h. During the entire exposure time the coating protected the austenitic base material.

CRediT authorship contribution statement

Annette Heinzel: Writing – original draft, Investigation, Conceptualization. **Renate Fetzer:** Writing – review & editing, Investigation. **Fabian Lang:** Investigation. **Alfons Weisenburger:** Writing – review & editing, Supervision, Funding acquisition, Conceptualization. **Sebastiano Cataldo:** Resources. **Fabio Di Fonzo:** Resources. **Georg Müller:** Project administration.

Declaration of competing interest

The authors declare that they have no known competing financial interests or personal relationships that could have appeared to influence the work reported in this paper.

Data availability

The raw/processed data required to reproduce these findings cannot be shared at this time due to technical or time limitations. The data are available from the corresponding author on reasonable request.

Acknowledgements

The authors would like to thank the Centre for Nano-Science and Technology (CNST @PoliMi, Milan) of the Istituto Italiano di Tecnologia and the ENEA-FSN-ING Division, C.R. Brasimone for providing the PLD and DG coated samples and the Belgian Nuclear Research Centre (SCK-CEN) for providing oxygen sensors with Bi/Bi_2O_3 reference used in the CORELLA facility. The work was carried out in the frame of EERA Joint Programme Nuclear Materials and is partly funded by the European Commission HORIZON 2020 Framework Programme under grant agreement no. 755269, the GEMMA (Generation IV Materials Maturity) H2020 program.

References

[1] A. Heinzel, W. Hering, J. Konys, L. Marocco, K. Litfin, G. Mueller, J. Pacio, C. Schroer, R. Stieglitz, L. Stoppel, A. Weisenburger, T. Wetzel, Liquid metals as efficient high-temperature heat-transport fluids, Energy Technol. 5 (2017) 1026–1036.
[2] D. Frazer, E. Stergar, C. Cionea, P. Hosemann, Liquid metal as a heat transport for thermal solar power applications, Energy Procedia 49 (2014) 627–636.
[3] Y. Wu, Design and R&D progress of China lead-based reactor for ADS research facility, Engineering 2 (2016) 124–131.
[4] A. Alemberti, The lead fast reactor: an opportunity for the future? Engineering 2 (2016) 59–62.
[5] F.J. Martín-Muñoz, 6. Compatibility of structural materials with lead-bismuth eutectic and lead: standardisation of data, corrosion mechanism and rate, in: Handbook on Lead-Bismuth Eutectic Alloys and Lead Properties, Materials Compatibility, Thermal-Hydraulics and Technology - 2015 Edition, 7268, OECD, NEA, 2015.
[6] A. Weisenburger, C. Schroer, A. Jianu, A. Heinzel, J. Konys, G. Müller, C. Fazio, A. Gessi, S. Babayan, A. Kobzova, L. Martinelli, K. Ginestar, F. Balbaud-Célerier, F. J. Martín-Muñoz, L. Soler Crespo, Long term corrosion on T91 and AISI 316L steel in flowing lead alloy and corrosion protection barrier development, J. Nucl. Mater. 415 (2011) 260–269.
[7] F.G. Ferré, E. Bertarelli, A. Chiodoni, D. Carnelli, D. Gastaldi, P. Vena, M.G. Beghi, F. Di Fonzo, The mechanical properties of a nanocrystalline Al_2O_3/α-Al_2O_3

composite coating measured by nanoindentation and Brillouin spectroscopy, Acta Mater. 61 (2013) 2662–2670.
[8] F.G. Ferré, M. Ormellese, F. Di Fonzo, M.G. Beghi, Advanced Al_2O_3 coatings for high temperature operation of steels in heavy liquid metals: a preliminary study, Corros. Sci. 77 (2013) 375–378.
[9] F.G. Ferré, A. Mairov, D. Vanazzi, S. Bassini, M. Utili, M. Tarantino, M. Bragalia, F. R. Lamastra, F. Nanni, L. Ceseracciu, Y. Serruys, P. Trocellier, L. Beck, K. Sridharan, M.G. Beghi, F. Di Fonzo, Corrosion and radiation resistant nanoceramic coatings for lead fast reactor, Corros. Sci. 124 (2017) 80–92.
[10] A. Zaborowska, L. Kurpaska, E. Wyszkowska, M. Clozel, M. Vanazzi, F. Di Fonzo, M. Turek, I. Jóźwik, A. Kosińska, J. Jagielski;, Influence of ion irradiation on the nanomechanical properties of thin alumina coatings deposited on 316L SS by PLD, Surf. Coat. Technol. 386 (2020) 125491.
[11] I.P. Serre, I. Ponsot, J.-B. Vogt, Alumina-Forming Austenitic (AFA) steels and aluminium-based coating on 15-15 Ti steel to limit mechanical damage in presence of liquid lead-bismuth eutectic and liquid lead, MATEC Web Conf. 349 (2021) 02007.
[12] GEMMA projects (https://cordis.europa.eu/project/id/755269/results/de-Evaluationofmitigationtechniquesagainstliquidmetalcorrosioninheavyliquidmetals).
[13] P. Saravanan, V. Selvarajan, D.S. Rao, S.V. Joshi, G. Sundararajan, Influence of process variables on the quality of detonation gun sprayed alumina coatings, Surf. Coat. Technol 123 (2000) 44–54.
[14] Y. Wang, Friction and ear performances of detonation gun- and plasma-sprayed ceramic and cermet hard coatings und dry friction, Wear 161 (1993) 69–78.
[15] R.C. Tucker Jr., Detonation gun coatings, JOM 38 (1986) 66–67.
[16] M. Chocholousek, L. Rozumova, Z. Spirit, F. Di Gabriele, Coating on steels T91 and 316L in lead-bismuth eutectic environment, in: 461, 2019 012028.
[17] A. Jianu, R. Fetzer, A. Weisenburger, S. Doyle, M. Bruns, A. Heinzel, P. Hosemann, G. Mueller, Stability domain of alumina thermally grown on Fe-Cr-Al-based model alloys and modified surface layers exposed to oxygen-containing Pb, J. Nucl. Mater. 470 (2016) 68–75.
[18] V. Engelko, B. Yatsenko, G. Müller, H. Bluhm, Pulse electron beam facility (GESA) for surface treatment of materials, Vaccum 62 (2001) 211–216.
[19] A. Weisenburger, A. Heinzel, G. Müller, A. Roussanov, T91 cladding tube with and without modified FeCrAlY coatings exposed in LBE at different flow, stress and temperature conditions, J. Nucl. Mater. 376 (2008) 274–281.
[20] S. Takaya, T. Furukawa, G. Müller, A. Heinzel, A. Jianu, A. Weisenburger, K. Aoto, M. Inoue, F.Abe T.Okuda, S. Ohnuki, T. Fujisawa, A. Kimura, Al-containing ODS steels with improved corrosion resistance to liquid lead-bismuth, J. Nucl. Mater. 428 (2012) 125–130.
[21] V. Engelko, G. Mueller, A. Rusanov, V. Markov, K. Tkachenko, A. Weisenburger, A. Kashtanov, A. Chikiryaka, A. Jianu, Surface modification/alloying intense pulsed electron beam as a tool for improving the corrosion resistance of steels exposed to heavy liquid metals, J. Nucl. Mater. 415 (2011) 270–275.
[22] Ph. Deloffre, F. Balbaud-Célérier, A. Terlain, Corrosion behaviour of aluminized martensitic and austenitic steel in liquid Pb-Bi, J. Nucl. Mater. 335 (2004) 180–184.
[23] J. Van den Bosch, A. Almazouzi, EUROTRANS-DEMETRA-Task 4.1.2: reference materials procurement, dispatching and characterization, procurement and characterizatioin of T91 and SS316L Plates, SCK*CEN, Mol, Belgium, Technical Report No. SCK*CEN-R-4197, 2005.
[24] V. Tsisar, C. Schroer, O. Wedemeyer, A. Skrypnik, J. Konys, Effect of structural state of austenitic 15-15Ti steel on initiation and propagation of solution-based corrosion attack in flowing liquid Pb-Bi eutectic at 400 and 500 °C, in: Proceedings of the 25th International Conference on Nuclear Engineering ICONE25, Shanghai, China, 2017, https://doi.org/10.1115/ICONE25-66634.
[25] K. Lambrinou, E. Charalampopoulou, T. Van der Donck, R. Delville, D. Schryvers, Dissolution corrosion of 316L stainless steels in contact with static liquid lead-bismuth eutectic (LBE) at 500 °C, J. Nucl. Mater. 490 (2017) 9–27.
[26] G. Müller, G. Schumacher, A. Weisenburger, A. Heinzel, F. Zimmermann, T. Furukawa, K. Aoto, Study on Pb/Bi corrosion of structural and fuel cladding material for nuclear application, Part I, JNC TY 9400 2002-016.
[27] G. Müller, A. Heinzel, G. Schuhmacher, A. Weisenburger, Control of oxygen concentration in liquid lead and lead-bismuth, J. Nucl. Mater. 321 (2003) 256.
[28] L. Martinelli, S. Gossé, P. Agostini, F. Balbaud-Célérier, A. Ciampichetti, J.-L. Courouau, N. Li, H. Glasbrenner, V.P. Sobolev, A. Terlain, 3. Thermodynamic relationship and heavy liquid metal interaction with other coolants, in: Handbook on Lead-Bismuth Eutectic Alloys and Lead Properties, Materials Compatibility, Thermal-Hydraulics and Technology - 2015 Edition, 7268, OECD, NEA, 2015.
[29] P. Lorusso, S. Bassini, A. Del Nevo, I. Di Piazza, F. Giannetti, M. Tarantino, M. Utili, GEN-IV LFR development: status & perspectives, Prog. Nucl. Energy 105 (2018) 318–331.
[30] M. Kieser, H. Muscher, A. Weisenburger, A. Heinzel, G. Müller, Liquid metal corrosion/erosion investigations of structure materials in lead cooled systems: part 1, J. Nucl. Mater. 392 (2009) 405–412.
[31] R. Fetzer, A. Weisenburger, G. Müller, Turbulent flow of liquid lead alloy in oxygen-controlled corrosion erosion test facility, AIP Adv. 11 (2021) 075303.
[32] G. Müller, G. Schumacher, A. Heinzel, A. Jianu, A. Weisenburger, 9. Corrosion protection in lead and lead bismuth eutectic at elevated temperatures, in: Handbook on Lead-Bismuth Eutectic Alloys and Lead Properties, Materials Compatibility, Thermal-Hydraulics and Technology - 2015 Edition, 7268, OECD, NEA, 2015.
[33] F. Azarmi, X.M. Tangpong, Evaluation of microstructural characteristics in alumina produced by selective laser stereolithography and detonation gun spraying, Metallogr., Microstruct., Anal. 9 (2020) 503–510.
[34] N. Kantay, B. Rakhadilov, S. Kurbanbekov, D. Yeskermessov, G. Yerbolatova, A. Apsezhanova, Influence of detonation-spraying parameters on the phase composition and tribological properties of Al_2O_3 coatings, Coatings 11 (2021) 793.
[35] C. Houngniou, S. Chevalier, J.P. Larpin, High-temperature-oxidation behaviour of iron–aluminide diffusion coatings, Oxid. Metals 65 (2006) 409–439.
[36] K.M.N. Prasanna, A.S. Khanna, R. Chandra, W.J. Quadakker, Effect of θ- alumina formation on the growth kinetics of alumina-forming superalloys, Oxid. Metals 46 (1996) 465–480.